CLAP4CLIP: Continual Learning with Probabilistic Finetuning for Vision-Language Models

Saurav Jha[1], **Dong Gong**[1*], **Lina Yao**[1,2]
[1]University of New South Wales (UNSW Sydney), [2]CSIRO's Data61
{saurav.jha, dong.gong}@unsw.edu.au; lina.yao@data61.csiro.au

Abstract

Continual learning (CL) aims to help deep neural networks learn new knowledge while retaining what has been learned. Owing to their powerful generalizability, pre-trained vision-language models such as Contrastive Language-Image Pre-training (CLIP) [1] have lately gained traction as practical CL candidates. However, the domain mismatch between the pre-training and the downstream CL tasks often calls for finetuning of the CLIP on the latter. Most existing finetuning methods exhibit deterministic nature. This makes them overlook the many possible interactions across the input modalities and deems them unsafe for high-risk tasks requiring reliable uncertainty estimation. To address these, our work proposes **C**ontinual **LeA**rning with **P**robabilistic finetuning (CLAP) - a probabilistic modeling framework over visual-guided text features per task, thus providing more calibrated CL finetuning. Unlike recent data-hungry anti-forgetting CL techniques, CLAP alleviates forgetting by exploiting the rich pre-trained knowledge of CLIP for weight initialization and distribution regularization of task-specific parameters. Cooperating with the diverse range of existing prompting methods, CLAP can surpass the predominant deterministic finetuning approaches for CL with CLIP. We conclude with out-of-the-box applications of superior uncertainty estimation abilities of CLAP including novel data detection and exemplar selection within the existing CL setups. Our code is available at `https://github.com/srvCodes/clap4clip`.

1 Introduction

Learning in the real world involves dealing with the ever-changing distributions of task streams and their data [2, 3, 4]. Given the constraints on resources and privacy, there is also no guarantee for re-training a network on all previously seen data [5]. Continual learning (CL) aims to learn from such data/task stream without *catastrophic forgetting* [6, 2] of past data/tasks. A challenging CL setup is the class-incremental learning setting, where new classes emerge with new tasks, and at test time, a model must infer from all seen classes without known task IDs [7, 8].

Recent years have seen pre-trained multi-modal foundation models excel on several domains [1, 9, 10]. One such example for the vision-language (VL) domain is the CLIP [1] model that comes with strong zero-shot generalizability acquired by learning to match large-scale image-text pairs in a contrastive manner [11]. However, to adapt well to downstream tasks, CLIP must be finetuned on the task-specific data [12, 13]. Considering both the need for continually finetuning pre-trained models on streaming tasks and their perks over training from scratch [14], our work studies CL with CLIP.

An issue with the existing deterministic approaches to finetuning [13, 12] is that these overlook the *uncertainties* arising from many possible interactions between the visual and textual cues of downstream tasks. For instance, on the textual side, while a good generic hand-crafted prompt for images is "`A photo of a {class}`", there can be instances where further tailored prompts help

*Corresponding author

38th Conference on Neural Information Processing Systems (NeurIPS 2024).

 https://doi.org/10.52202/079017-4102

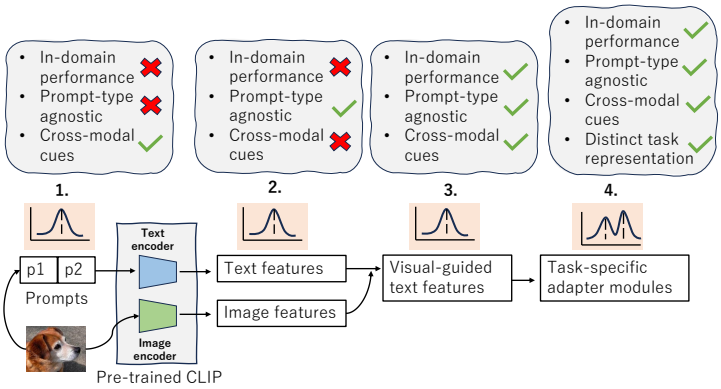

Figure 1: **Concept diagram for probabilistic finetuning of pre-trained CLIP in a CL setup:** We identify four such suitable design choices for probabilistic modelling. Choice #1 [17] performs variational modelling by imposing prior on the prompt space which makes it prompt-type dependent while also interfering with the in-domain knowledge learning capability of the prompts – a criterion crucial in the deployment of CL models. Choice #2 (see Sec. 3.2.1) instead imposes a prior on the outputs of the text encoder. While this makes it prompt-type agnostic (as the text features can now be derived from arbitrary prompt types), not taking the visual information into account nevertheless leads to the loss of information about cross-modal interactions between the visual and textual cues – a property essential for preventing cross-modal deviation of finetuned features in CL (see Sec. 3.2.2). Choice #3 (Ours) leverages the best of both worlds by modelling the distribution of visual-guided text features. To further refine the learned distributions of CL tasks, we finally introduce lightweight task-specific adapter modules in choice #4 that make the cross-task centroids more distinct while preserving the aforesaid properties (see Sec. 3.2.3).

improve the image-to-text coherence. Similarly, on the visual side, images from the same class can have diverse range of backgrounds, poses, orientations, etc. Overlooking the uncertainties in image-text matching can thus cause overfitting on downstream tasks and forgetting of the generalizable knowledge [15]. For CL, where we seek to adapt CLIP on a stream of tasks, this can further lead to the cross-modal features increasingly deviating from each other to the point of catastrophic forgetting (see Fig. 3b). While existing methods [16, 17] model such uncertainties through probabilistic finetuning, these remain subpar at CL given: (a) their inaptness to leverage existing prompt-based approaches [16], (b) their excessive trading of in-domain performance for generalization [17].

Lastly, like other autonomous real-world agents, CL models deployed in mission-critical settings (healthcare, transport, etc.) can benefit from uncertainty awareness by calibrating their predictions to reliably assess their confidences [18, 8]. Hence, to enhance the usage of the pre-trained CLIP for real-world CL tasks, we design a finetuning approach with the following three properties (see Fig. 1): A) **probabilistic modeling** of cross-modal task cues for better generalization; B) **compatibility** with prompt-based finetuning methods [14, 12, 19, 20] to exploit their finegrained in-domain task knowledge; C) leveraging the **rich pre-trained knowledge** of CLIP to further counter forgetting.

To this end, we design a principled Variational Inference (VI) framework that learns the functional space of task-specific posterior distributions based on text features that are aligned with their visual counterpart (property #**A**). To refine these variational task posteriors, we draw our motivation from Bayesian mixture-of-experts ensembles [21, 22], and employ lightweight task-specific adapter modules that model task-specific distributions. Our final prediction is thus a mixture of logits derived from individual task adapter modules. To further counter the forgetting in these modules, we diverge from the recent trend of internet data-hungry CL techniques [23, 24]. Instead, we exploit the readily available pre-trained language knowledge of CLIP for weight initialization and task distribution regularization (property #**C**). Finally, by modelling the distribution of the text feature space, our probabilistic finetuning method boasts a rich modular nature as the features can be derived from arbitrary prompt types (property #**B**). In particular, we show that our framework can inherit the in-domain knowledge of hand-crafted [1], uni-modal [12], multi-modal [20], or instance-conditioned [19] prompts. We backronymize our finetuning approach as **CLAP** – **C**ontinual **LeA**rning with **P**robabilistic finetuning – for the pre-trained CLIP model. Our experiments across

https://doi.org/10.52202/079017-4102

several settings show that CLAP4CLIP enhances *prompt-based* finetuning for CLIP, and surpasses the predominant deterministic finetuning methods in terms of in-domain performance, output calibration, and generalization to unseen CL tasks, all while sharing a similar resource overhead. We study some out-of-the-box perks of CLAP's probabilistic nature by leveraging its uncertainty estimation capabilities on a proposed *post-hoc* novel data detection setup and on exemplar selection for CL.

2 Related work

Continual Learning (CL). The existing CL literature is predominated by three categories of methods: (a) Regularization-based methods [6, 25, 26] alleviate forgetting by punishing changes to the parameters that are important to previous tasks; (b) Architecture-based approaches learn parameters that are specialized for individual tasks either by network expansion [27] or by sub-network composition [28, 29]; (c) Rehearsal-based approaches [30, 5] rely on storing a fraction of the past task experiences in a memory to train with the current task. Each category has its own flaw – methods in (a) struggle to discriminate inter-task classes [31]; those in (b) often require task oracle during inference; those in (c) are sensitive to the memory sizes besides being prone to overfitting on the memory samples [32]. Hence, practical CL calls for combining these. Our work leverages (a) via function-space regularization (Sec. 3.4), (b) via task-specific modules (Sec. 3.2.3), and (c) via herding-based replay (see App. A.1.1).

Vision-Language Models (VLMs) finetuning. The powerful generalizability of pre-trained VLMs [9, 33] like the CLIP [1] has enabled their zero-shot applications to a range of downstream tasks, including CL [14]. In practice, their performance on downstream out-of-domain data remains rather weak [34, 35]. For such cases, finetuning on task-specific data is a natural choice. Instead of performing extensive *full finetuning* on all parameters, some *parameter-efficient finetuning* (PEFT) methods learn a lightweight feature adapter module for textual and/or visual paths [13, 36]. Another line of PEFT methods learns *soft prompts* which are a few continuous tokens serving as inputs to the frozen visual and/or textual encoder(s) to capture task-specific information [12, 37, 20]. Existing works on CL with pre-trained CLIP have leveraged either [19, 38] or both [39] of these methods. However, such finetuning methods remain deterministic in nature. This imposes an explicit constraint on the modeling of the possible ways in which the visual and the textual semantics interact.

To address the aforesaid flaw, one could turn to adapt the existing probabilistic finetuning approaches to capture the cross-modal interactions in CL tasks. For instance, [16] learn the distribution of hand-crafted prompts while [17] propose variational prompt tuning (VPT) *conditioned* on the input images. Yet these methods are limited in their efficacy. [16] is incompatible with conditional prompt learning [37], which is an extensively studied PEFT field. VPT [17] trades in-domain performance excessively in favor of generalizability – a trait detrimental in the deployment of CL models. Our work aims to bridge these gaps for probabilistic finetuning all while adapting it for CL.

3 Methodology

3.1 Preliminaries

Continual Learning (CL). Class-incremental CL [7] aims to learn from a sequence of T tasks $[(C^1, D^1), (C^2, D^2), ..., (C^T, D^T)]$. Each task $t \in [1, T]$ has its training data $D^t = \{(\mathbf{x}_1, y_1), (\mathbf{x}_2, y_2), ..., (\mathbf{x}_{k^t}, y_{k^t})\}$, where $\mathbf{x}$ and y are the input images and labels, respectively from the set of classes $C^t = \{c_1^t, c_2^t, ..., c_{n^t}^t\}$. Following [40, 41], we assume any two task-specific sets of classes to be disjoint: $C^i \cap C^j = \emptyset$. A neural network with parameters ϕ is then trained on task t using D^t to minimize the cross-entropy loss over C^t. At test time, the model is evaluated on all seen classes $C = \bigcup_{i=1}^{t} C^i$, where the past task predictions are prone to forgetting. As a solution, rehearsal-based methods [42, 43] replay past task samples from a memory $\mathcal{M}$ during training. Following [30], we use herding [44] to maintain $\mathcal{M}$ (see App. A.1.1 for details).

CLIP with prompt. CLIP comprises an image encoder $f(\mathbf{x})$ acting on an image $\mathbf{x} \in \mathbb{R}^{3\times H\times W}$ of height H and width W, and a text encoder $g(\mathbf{t}(\mathbf{p}))$ acting on a word embedding vector $\mathbf{t} \in \mathbb{R}^{(L\times e)}$ derived from a text prompt $\mathbf{p} \in \mathbb{R}^{((L-1)\times e)}$. Here, L is the text length, and e is the text embedding dimension. The encoders's outputs are used in the prediction of the class y_i as:

$$p(y_i|\mathbf{x}) = \frac{\exp\left(\langle f(\mathbf{x})^T, g(\mathbf{t}_i)\rangle/\tau\right)}{\sum_{c=1}^{|C^t|}\exp\left(\langle f(\mathbf{x})^T, g(\mathbf{t}_c)\rangle/\tau\right)}, \tag{1}$$

where τ is a learnable temperature parameter, $\langle\cdot,\cdot\rangle$ is the cosine similarity, and the c-th class text feature $\mathbf{t}_c = [\mathbf{p}, \mathbf{e}_c]$ is the result of adding a class-specific word embedding $\mathbf{e}_c$ to the prompt $\mathbf{p}$. The

 https://doi.org/10.52202/079017-4102

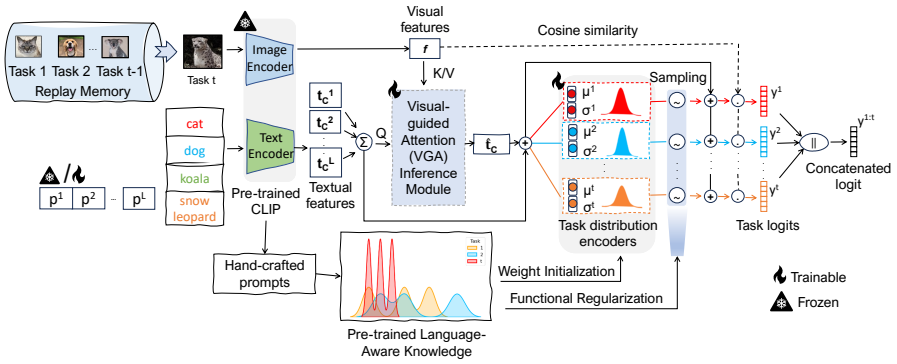

Figure 2: **CLAP4CLIP overview:** the visual-guided attention (VGA) inference module uses the text features as query (Q), and the visual features as keys (K) and values (V) to produce visual-guided text features. The task-specific text features are fed to their respective task distribution encoders (μ^t, σ^t). The task distribution samples are then fused with the original task features prior to deriving the task logits y^t. All task logits are concatenated to produce the final prediction $y^{1:t}$.

features $g(\mathbf{t}_c)$ for all classes are used as the weights of a linear classifier. In CL, $g(\mathbf{t}_c)$ would thus encode the features for classes $c \in C$ seen until task t. Eq. (1) forms a contrastive training criterion for the text and visual modalities, whose rich representation allows pre-trained CLIP to be used for zero-shot classification through *hard* prompt templates, *i.e.,* $\mathbf{p}^c =$ "`A photo of a {c`$^{\text{th}}$ `class}`".

CLIP finetuning with learnable soft prompts. To improve the CLIP performance on a downstream task t, *soft* prompts use a set of learnable vector tokens $\mathbf{p} = \{\mathbf{p}^1, \mathbf{p}^2, ..., \mathbf{p}^L\}$. CoOp [12] shares $\mathbf{p}$ with all classes of a task. MaPLe [20] learns multi-modal prompts by employing two such token sets $\mathbf{p}_f$ and $\mathbf{p}_g$ until the J-th layers of the vision and the text encoders of CLIP, respectively. AttriCLIP [19] selects a subset of prompts conditioned on the input: $\{\{\mathbf{p}^j\}_{1 \leq j \leq L} | \mathbf{x}_k\}$. Learning $\mathbf{p}$ (with frozen CLIP weights) thusly helps encode task/modality/instance-conditioned context for a given task.

CLIP finetuning with adapters. Adapter-based methods like CLIP-Adapter [13] learn lightweight modules over text and/or visual features of the frozen CLIP model. With a text adapter A_t, the updated text features from Eq. (1) can be rewritten (with a slight abuse of notation) as:

$$g(\mathbf{t}_i) = \alpha A_t(g(\mathbf{t}_i)) + \beta g(\mathbf{t}_i), \tag{2}$$

where α and β control the strength of the residual connection between the adapted and the pretrained models' features, e.g., $\beta = 1 - \alpha$ in [13].

3.2 CL with probabilistic finetuning for CLIP

Overview. We develop our CLIP-based probabilistic finetuning model using a Bayesian VI framework (see Fig. 2). Sec. 3.2.1 starts by making the case that, unlike previous VI-based finetuning approaches, the feature embedding space of the text encoder output is a superior choice for defining our functional space priors on. While linear adapter layers are often employed for obtaining the mapping from such a pre-defined feature-space prior to the function outputs [45, 17], we show in Sec. 3.2.2 that CL finetuning with generic adapter leads to the issue of cross-modal deviation. In Sec. 3.2.3, we then propose refining our variational distribution on function space using an ensemble of task-specific adapters that are built on top of cross-modal aligned text features.

3.2.1 Variational inference with function space prior on text features

We are interested in modeling the stochastic processes that generate the labels y for the inputs $\mathbf{x}$ of a CL task t. To this end, we assume a prior distribution p_χ over the text feature of the c-th class: $p_\chi(\mathbf{t}_c(\mathbf{p}))$. We can then draw M number of latent variables $z = \{z_m \sim p_\chi\}_{m=1}^M$ to represent the c-th class text feature $\mathbf{t}_c(\mathbf{p})$ as a linear combination of the text encoder feature $g(\mathbf{t}_c(\mathbf{p}))$ and z:

$$\mathbf{t}_c(\mathbf{p}) = \{g(\mathbf{t}_c(\mathbf{p})) + z_m\}_{m=1}^M, \quad \text{s.t. } z_m \sim p_\chi, \tag{3a}$$

$$p(y_i|\mathbf{x}) = \int_\chi \frac{\exp\left(\langle f(\mathbf{x})^T, \mathbf{t}_c(\mathbf{p})\rangle\right)}{\sum_{c=1}^{|C^t|} \exp\left(\langle f(\mathbf{x})^T, \mathbf{t}_c(\mathbf{p})\rangle\right)} p(\mathbf{t}_c(\mathbf{p}))d\chi, \tag{3b}$$

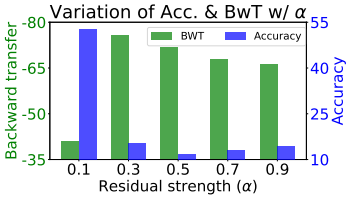

(a) Effect of α on Accuracy and Backward Transfer (BwT).

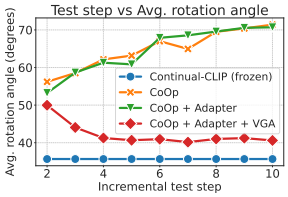

(b) Avg. rotation angle [47] per incremental step for image and text features.

Figure 3: **Need for Visual-guided Attention (VGA) inference module.** Fig. 3a: A simple adapter is inadequate at preventing catastrophic forgetting in CL – marked by high BwT scores; Fig. 3b: VGA module encourages cross-modal alignment between the learned text features and the pre-trained visual features – marked by a decrease in average angle $\texttt{arccos}\langle t, 1\rangle$ between them – where otherwise the former deviates further with incremental training steps.

where Eq. (3b) replaces $g(\mathbf{t}_i)$ in Eq. (1) by $\mathbf{t}_c(\mathbf{p})$. Eq. (3b) thus results into M number of predictions whose distribution gives us the model's epistemic uncertainty about the correct prediction. To deal with the intractability of the marginal likelihood, we optimize for the evidence lower bound (ELBO) using a variational posterior q_ϕ that approximates the prior p_χ based on the KL-divergence loss $\mathbb{D}_{\text{KL}}$:

$$\log p(y|\mathbf{x}) \geq \mathbb{E}_{q_\phi(z|\mathbf{t}_c)}[\log p(y|\mathbf{x}, z)] - \mathbb{D}_{\text{KL}}\big(q_\phi(z|\mathbf{t}_c)\|p_\chi\big). \tag{4}$$

By assuming p_χ to be the (static) standard Gaussian $\mathcal{N}(\mathbf{0}, \mathbf{I})$ and q_ϕ to be the (learnable) Gaussian $\mathcal{N}(\mu(\mathbf{t}_c), \sigma(\mathbf{t}_c))$, whose mean μ and standard deviation σ are parameterized by linear adapter layers, we can ensure that the random variable z remains differentiable by reparameterization trick [45]. Accordingly, we refer to the parameters $[\mu; \sigma]$ together as *probabilistic adapter* from here onward.

Imposing the prior over the text feature offers us *further advantages* over that in the prompt embedding space as done by VPT [17] (also see App. Fig. 1 for an illustration). First, Eq. (3b) is prompt-type agnostic as the text features $g(\mathbf{t})$ could be derived from any existing soft [37, 19, 20] or hard [14, 13] prompts.[2] Second, by leaving the prompt embedding space intact and injecting stochasticity into the feature space, we can better learn the task-specific knowledge known to be encoded by the prompt embeddings [46]. This can help bypass the loss of in-domain performance. In CL, the latter property is crucial for our model to perform well on all previously seen tasks. Third, as the latent variable z is now directly used to infer the logits, it naturally favors generalization by influencing the predictions. On the contrary, the effect of the prompt space prior on the predictions is indirect as it is mediated by the representations of the entire text encoder layers. This can make the influence of the prior harder to control and can hinder the aforesaid interpretability in the model's predictions.

Efficient continual finetuning with a probabilistic adapter. Finetuning adapters for CL is not straightforward. Namely, we have the overhead of searching for task-specific residual ratio α (see Eq. (2)) which is sensitive to the training setup including dataset and prompt-type [13, 36]. This has particularly worse implications for a probabilistic adapter like ours, where a larger α can inject enough noise to corrupt the pre-trained representations to the point of catastrophic forgetting (see Fig. 3a). For efficient learning of our adapter, we thus seek to retain *no additional overhead* of hyperparameter search for the residual ratio. Subsequently, we use $\alpha = \beta = 1$ through our work.

3.2.2 Cross-modal feature deviation in continual finetuning of CLIP

To perform CL with variational modelling in the text feature space, we first take a step back to investigate how CL in general affects the *cross-modal deviation* [47] between the learned text and the frozen visual features of finetuning methods. To this end, we consider two basic CL models: the CoOp [12] and the CoOp with a CLIP-Adapter [13]. Then, for the base task ($t = 1$) test samples of CIFAR100, we compute the average of the Rotation Angle Matrix (RAM) [47] using the CL models' frozen visual $f(\mathbf{x})$ and learnable textual $g(\mathbf{t}_c(\mathbf{p}))$ features at each incremental test step. Fig. 3b shows the deviation of the learned textual features from their (frozen) visual counterparts for the CoOp. This implies that the cross-modal retrieval performance of CLIP finetuned with learnable prompts deteriorates with incremental training. Moreover, as a generic adapter (CoOp + Adapter) does not remedy the cross-modal deviation, this sets a direct hindrance in employing our probabilistic adapter to learn the variational distribution q_ϕ.

[2]From a practitioner's perspective, this enriches the modularity by taking away the overhead of engineering the priors specific to the prompt-type that could, for instance, be spanning multiple layers and/or modalities.

https://doi.org/10.52202/079017-4102

Variational modeling on visual-guided text features. For variational modeling of text features $\mathbf{t}_c(\mathbf{p})$ that remain aligned with the visual features during continual finetuning, we propose enriching the text features with the visual context through an explicit attention mechanism (see App. A.3 for further justification on this design choice). To this end, we treat the text features as queries Q and the visual features as keys K and values V, and adopt a standard transformer-styled decoder block [48] as a task-shared Visual-guided attention (VGA) module. The VGA module performs text-to-text self-attention followed by text-to-visual cross-attention. To eliminate the influence of the text features from multiple CL tasks, a *naive* strategy is to perform specialized VGA forward passes with task-specific queries [27]. We seek to replace several such costly VGA passes with a single pass. To do so, we exploit the global nature of our visual context and mask out (set to $-\infty$) all inter-task connections in the queries using a target mask. This ensures that only the task-specific text features undergo self-attention while the entire query still attends to the visual context:

$$\{\hat{\mathbf{t}}_c^k\}_{k=1}^t = \text{VGA}\big(Q = \{\mathbf{t}_c^k\}_{k=1}^t, K = V = f(\mathbf{x})\big), \tag{5a}$$

$$\tilde{\mathbf{t}}_c^t = \hat{\mathbf{t}}_c^t + g(\mathbf{t}_c^t(\mathbf{p})), \tag{5b}$$

where $\hat{\mathbf{t}}_c^k$ is the task-specific visual-guided text feature which is fused with the residual task-specific text encoder feature $g(\mathbf{t}_c^t)$ to derive the task embedding $\tilde{\mathbf{t}}_c^t$. We note that in a non-CL setup, [49] employ the VGA module using the per-pixel spatial features (obtained before global average-pooling) instead of the globally pooled visual features of the ViT [50]. Our choice for the latter favors the efficiency of our framework for large CL datasets where attending to per-pixel spatial features can incur much higher latency (see App. A.4 for a comparison).

3.2.3 Task-specific probabilistic adapters as ensembles for posterior approximation

By exploring diverse modes in function space, ensembles of neural networks can better approximate the variational posterior [51, 22]. Motivated by this, we replace our task-shared adapter q_ϕ with task-specific adapters $\{q_\phi^i\}_{i=1}^t$ that parameterize the t-th task-specific posterior $\mathcal{N}(\mu^t, \sigma^t)$ over the task embeddings $\tilde{\mathbf{t}}_c^t$:

$$\{z_m^t\}_{m=1}^M \sim q_\phi^t(z|\tilde{\mathbf{t}}_c^t) = \mathcal{N}\big(\mu^t(\tilde{\mathbf{t}}_c^t), \sigma^t(\tilde{\mathbf{t}}_c^t)\big), \tag{6}$$

where z_m^t are the task-specific MC samples. Task-specific adapters thus serve as mixture-of-experts ensemble where each expert is trained on task-specific embeddings $\tilde{\mathbf{t}}_c^t$ and the logits computed using each expert is combined to derive the final prediction $\hat{y}^{1:t}$ (see Algo 1). The experts learn posteriors that are more discriminative across tasks. This is depicted in Fig. 4 using the cosine distance between the embeddings of the class-specific samples drawn from the posteriors. With task-specific adapters (right), the cross-task class centroids are more separable.

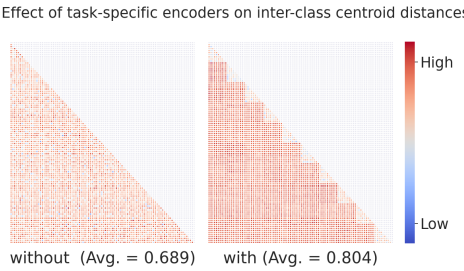

Figure 4: **Need for task-specific probabilistic adapters:** Cosine distance between the centroids of class-specific latent variables produced without (**left**) and with (**right**) task-specific adapters on CIFAR100 (10 tasks, 10 classes per task).

To prevent interference from current task training data, we freeze the past task encoders during each incremental training step ($t > 1$). Moreover, to reduce the forgetting in past task adapters, we follow other parameter-isolation techniques [27, 42, 52] to finetune on a class-balanced dataset of new data and rehearsal data $\mathcal{M}$ at the end of each incremental training step ($t > 1$). We refer to this as memory consolidation training (see App. A.2). We also provide an overview of a test-time forward pass of our framework in App. A.5.

Algorithm overview. App. algo. 1 outlines the pseudo-code of a forward pass of CLAP at $t-$th task test step. Here, a test image is to be classified into one of the classes $\{1, ..., |C^t|\}$. Our method executes the computationally heavy VGA layers only once. The task-specific VGA outputs are passed to their respective adapters. By limiting the quadratic complexity of the VGA pass, our method induces minimal time overhead. By only expanding the linear adapters per task, our memory overhead is negligible compared to the large backbone of the pre-trained CLIP model (ablation Fig. 5).

3.3 Alleviating forgetting with pre-trained language-aware CLIP knowledge

Like other finetuning methods, our probabilistic adapters are likely to trade the generalizability of text features for downstream task performances [12, 37]. On the contrary, the pre-trained CLIP text

encoder with hand-crafted prompts [53] has strong generalizability because of its rich pre-trained language information. We propose to leverage this pre-trained language knowledge to help guide the incremental finetuning in CLAP. In the following, we assume $\{\mathbf{t}_y^{h,l} \in \mathbb{R}^d\}_{l=1}^L$ to be the features corresponding to the L hand-crafted textual prompts for the class $y \in C^t$.

3.3.1 Past-task distribution regularization for mitigating forgetting

The functional spaces of the past task distributions are prone to forgetting in CL. Though replay helps alleviate the forgetting up to a certain degree, repeated training on the memory samples can lead to overfitting on these [32, 54]. To address this, previous works [8, 55] exploit functional priors for regularizing the visual space alongside memory replay. Here, we propose to regularize the past task distributions in the textual space by using the hand-crafted prompt-based features $\{\mathbf{t}_y^{h,l}\}_{l=1}^L$ to distill the past task latent samples $\left\{z^i = \{z_m^i\}_{m=1}^M\right\}_{i=1}^{t-1}$. Namely, the probability of the sample set z^t belonging to a class $y \in C^t$ is:

$$P_{\text{KD}}(y|z^t) = \frac{1}{M}\sum_{m=1}^{M}\frac{1}{L}\sum_{l=1}^{L}\frac{\exp\left(\langle \mathbf{t}_y^{h,l}, z_m^t\rangle\right)}{\sum_{c=1}^{|C^t|}\exp\left(\langle \mathbf{t}_c^{h,l}, z_m^t\rangle\right)}. \tag{7}$$

The resulting language-aware distillation loss is thus the sum of cross-entropy between the true label distribution y_c and the predicted probability distribution P_{KD} across all the past-task classes:

$$\mathcal{L}_{\text{KD}} = -\sum_{t=1}^{T-1}\sum_{c=1}^{|C^t|}\log P_{\text{KD}}(c|z^t)y_c, \tag{8}$$

where $\mathcal{L}_{\text{KD}}$ serves as a **data-free** (*i.e.*, no training samples required) text-to-text distribution regularizer that encourages the latent variable outputs from past-task adapters to stay close to the text features from the hand-crafted prompts. $\mathcal{L}_{\text{KD}}$ is applied only during the memory consolidation training, that is, when the past-task adapters are trainable. Lastly, as $\mathcal{L}_{\text{KD}}$ acts on the functional space of past tasks, this sets apart our setting from the non-CL setup of [56] where the language-aware distillation loss regularizes the vector embedding space.

3.3.2 Task-specific adapter initialization considering stability

Stability gap [57] in CL refers to the temporary yet substantial forgetting of past task knowledge in the initial phases of updating a network's weights to learn an incremental task. An informed weight initialization can help bridge this gap over random initialization by stabilizing the learning for new task components [58]. We thus leverage the $t-$th task text features $\{\mathbf{t}_y^{h,l}\}_{l=1}^L$ to initialize the weights $\mathbf{w}_t^\mu, \mathbf{w}_t^\sigma \in \mathbb{R}^{d\times d}$ of our $t-$th task's linear adapter layer. Let $\mathbf{s}_\mu, \mathbf{s}_\sigma \in \mathbb{R}^{|C^t|\times d}$ be the mean and the std. dev. of the L text features. We initialize $\mathbf{w}_t^\mu$ and $\mathbf{w}_t^\sigma$ as:

$$\mathbf{w}_t^\mu = \frac{1}{d}\langle \mathbf{s}_\mu^T, \mathbf{s}_\mu\rangle, \;\; \mathbf{w}_t^\sigma = \frac{1}{d}\langle \mathbf{s}_\sigma^T, \mathbf{s}_\sigma\rangle. \tag{9}$$

3.4 Training objective

Approximate ELBO. Building upon Eq. (4), we now learn the task-specific adapters q_ϕ^t to approximate the intractable $t \in [1, T]$ task-specific posteriors. The ELBO (see App. F for derivation) is:

$$\log p(y^{1:T}|\mathbf{x}; \tilde{\mathbf{t}}_c^t) \geq \sum_{t=1}^{T}\left[\mathbb{E}_{q_\phi^t(z^t|\mathbf{x};\tilde{\mathbf{t}}_c^t)}\left[\log p_\theta(y^t|z^t, \mathbf{x}; \tilde{\mathbf{t}}_c^t)\right] - \mathbb{D}_{\text{KL}}\big(q_\phi^t(z^t|\mathbf{x}; \tilde{\mathbf{t}}_c^t)\|p_\chi(z^t)\big)\right]. \tag{10}$$

Overall objective. Denoting the loss weights by λ and γ, our total loss term can be given as $\mathcal{L} = \mathcal{L}_{\text{CE}} - \lambda\mathbb{D}_{\text{KL}} + \gamma\mathcal{L}_{\text{KD}}$, where the cross-entropy $\mathcal{L}_{\text{CE}}$ and the prior-matching $\mathbb{D}_{\text{KL}}$ terms act on the outputs of all task encoders while the distribution regularization term $\mathcal{L}_{\text{KD}}$ acts only on the past task encoders. λ is set to 0.001. As the past task encoders are trainable only during the memory consolidation training stage, λ for these is set to 0 during training. γ is set to 15.

4 Experiments

Datasets. We evaluate our method on CIFAR100 [3, 30], ImageNet100 [41, 43], ImageNet-R [59], CUB200 [60], and VTAB [60]. CIFAR100 [61] and ImageNet100 [62] setups split their respective original datasets into 10 tasks with 10 classes each. ImageNet-R [63] and CUB200 split 200 classes

 https://doi.org/10.52202/079017-4102

Method	CIFAR100		ImageNet100		ImageNet-R		CUB200		VTAB	
	Avg ↑	**Last** ↑	**Avg** ↑	**Last** ↑	**Avg** ↑	**Last** ↑	**Avg** ↑	**Last** ↑	**Avg** ↑	**Last** ↑
Single-task JOINT	80.28		81.08		80.92		75.4		89.29	
Task-specific JOINT	82.9		83.55		83.07		85.72		94.6	
iCaRL [30]	72.93	57.6	68.62	59.5	66.34	43.71	82.39	75.1	53.38	41.6
L2P [65]	78.92	70.04	-	-	77.07	69.33	76.98	68.47	-	-
DualPrompt [59]	82.11	74.31	-	-	82.73	76.41	82.37	76.29	-	-
CODA-P [38]	85.19	76.4	85.93	79.02	82.06	79.5	84.77	80.39	87.5	81.2
PROOF [39]	84.84	76.55	-	-	84.89	79.7	83.98	79.35	-	-
Continual-CLIP [14]	78.65	68.26	83.99	74.2	84.43	76.94	67.0	54.8	68.5	60.97
CoOp [12]	81.17	70.58	79.14	64.9	84.7	78.66	76.62	68.53	87.06	81.25
MaPLe [20]	82.74	74.52	79.23	64.06	85.28	79.71	73.38	64.43	83.91	81.81
AttriCLIP [19]	79.31	68.45	82.29	70.76	83.09	76.53	65.26	52.12	71.84	64.09
CLIP-Adapter [13]	78.75	68.32	84.13	73.96	84.49	78.1	67.41	54.49	68.23	61.02
VPT [17]	73.4	59.33	80.51	61.09	81.66	74.0	69.14	60.03	67.2	77.26
Ours w/o VI	84.36	76.8	86.11	76.48	85.69	79.83	72.21	61.87	90.74	88.64
Ours	**86.13**	78.21	**87.76**	79.16	85.77	79.98	86.93	81.64	91.37	89.67
CoOp + Ours	85.71	77.4	86.8	78.18	85.32	79.52	**86.99**	**81.95**	**92.51**	**91.28**
MaPLe + Ours	86.06	**78.48**	87.47	79.02	86.25	80.56	81.53	74.24	90.97	88.83
AttriCLIP + Ours	78.06	67.59	87.37	**79.3**	**86.35**	**80.6**	83.71	79.01	74.84	71.12

Table 1: **Performance comparison** of different methods averaged over three runs. Best scores are in **bold**. The second-best scores are in blue. The results for L2P, DualPrompt, and PROOF are taken from [39]. See App. Table 12 for statistical significance of these results using std. dev. scores.

into 10 tasks with 20 classes each. VTAB has 5 tasks with 10 classes each [64]. While CIFAR100, ImageNet100, and CUB200 are robust settings for evaluating CL methods in the face of large forgetting, ImageNet-R and VTAB make challenging settings for CL methods using pre-trained models as these might include test images in their pre-training set (see App. A.1 for details).

Baselines. We compare CLAP4CLIP against several baselines and state-of-the-art finetuning methods. These include: (a) CLIP-based methods – Continual-CLIP [14], CoOp [12], CLIP-Adapter [13], AttriCLIP [19], MaPLe [20], and PROOF [39], (b) vision-only methods – DualPrompt [59] L2P [65], CODA-P [38], (c) the baseline CIL method – iCaRL [30]. For a fair comparison, we adhere to the experimental protocols of PROOF [39] throughout. We adopt ViT-B/16 with the pre-trained weights of OpenAI [1] as our backbone unless otherwise specified. As the upper bounds on performance, we use the CLAP4CLIP with single and task-specific encoders, trained on all tasks jointly (JOINT).

Variants. We integrate our method with four prompt-based approaches: Ours uses CLAP with hand-crafted prompt templates, CoOp + Ours with soft prompts [12], MaPLe + Ours uses multi-modal soft prompts [20], and AttriCLIP + Ours uses CLAP4CLIP with instance-conditioned soft prompts [19]. Ours w/o Variational Inference (VI) is the deterministic variant of Ours depicted in App. Fig. 7. We leave the details of the training and the hyperparameters of our models in App. A.2.

Performance measures. To quantify CL performances, we report: (a) the final accuracy after the last incremental step (Last) and the average of the accuracies after each step (Avg) [30], and (b) the backward transfer score (BwT) [66] to quantify forgetting. To assess the benefits of probabilistic modelling, we report: (a) the expected calibration error (ECE) [67] that measures the calibration in the model's predictions [68], and (b) the (forward) transfer score [69] that quantifies the generalizability of CL models by measuring the extent of their zero-shot transfer ability after finetuning.

4.1 Results

Accuracy. We report performances in Table 1 on all five datasets. Our method consistently achieves the best results among all the methods compared. Notably, on CIFAR100 and ImageNet100, our variants using the hand-crafted and multi-modal prompts outperform the others. On the challenging ImageNet-R setup with significant intra-class diversity, our method can better leverage the instance-conditioned prompt knowledge of AttriCLIP [19], which helps it outperform PROOF [39] by 1.46% in terms of average accuracy. On CUB200 and VTAB, sharing the prompt pool among all tasks gives CoOp [12] an edge over other baselines. Leveraging CoOp offers us the best results on these while surpassing PROOF, which also builds upon CoOp with task-specific soft prompts. We also observe that VPT [17] lags on all CL settings. Comparing the performance evolution of our variants against other baselines shows that our variants perform better throughout the incremental steps (App. Fig. 8).

Forgetting. Table 13 shows that in general, plugging CLAP4CLIP with prompt-based finetuning methods helps improve the BwT scores of the latter. It is worth noting that on the cross-dataset setting of VTAB [64], our variants are the only methods that effectively transfer the knowledge learned from

Method	ImageNet100	CIFAR100 + ImageNet100
DualPrompt [59]	81.9	67.1
Continual-CLIP [14]	75.4	54.9
CoOp [12]	79.3	55.4
MaPLe [20]	84.81	76.2
AttriCLIP [19]	83.3	78.3
PROOF [39]	81.26	82.59
Ours	83.51	83.83
CoOp + Ours	82	82.63
MaPLe + Ours	82.97	83.6
AttriCLIP + Ours	**84.14**	**84.56**

Table 2: **Performance comparison on the CDCL setting** [19]. All CLIP-based methods use the ViT-L/14 backbone.

ID	Probabilistic Encoder	VGA	Consolidation training	Task-specific Encoders	Weight Initialization	Distribution Regularization	Avg	Last
#1	✓						22.78	11.49
#2	✓	✓					82.82	73.41
#3	✓	✓	✓				84.4	74.99
#4	✓	✓	✓	✓			85.7	77.2
#5	✓	✓	✓	✓	✓		86.01	77.98
#6	✓	✓	✓	✓	✓	✓	86.13	78.21

Table 3: **Ablations** of the key components of CLAP4CLIP on CIFAR100.

incremental tasks to improve the performance on past tasks (*i.e.*, BwT > 0). This indicates that our probabilistic modeling strategy does not only counter forgetting but can also help bring anti-forgetting properties onto existing finetuning methods.

Calibration. App. Table 15 compares the ECE scores of our variants and their respective underlying deterministic baselines at the last test step. In general, our variants help enhance (decrease) the ECE scores of the underlying prompt-based methods. This implies that even in the face of forgetting in a CL setup, CLAP retains more reliability in assessing the confidence of its predictions.

Generalization. App. Table 14 shows that our method consistently enhances the (forward) transfer scores of the underlying deterministic prompt-based methods. This means that CLAP can better transfer the learned knowledge from seen tasks to help solve future tasks.

Resource-constrained CL. To study the robustness of CLAP towards memory and compute-constrained environments, we ablate its performance on *replay-free* [70] and *computationally-budgeted* [23] CL setups, respectively. Tables 16 and 17 show that for both these setups, leveraging the instance-conditioned and semantically diverse prompts of AttriCLIP provides an edge. Here, our variant leveraging AttriCLIP surpasses the replay-free SOTA, *i.e.,* CODA-P [38] and the budgeted SOTA, *i.e.,* AttriCLIP [19]. Further ablating the role of our proposed language-aware distribution regularization and weight initialization components for our AttriCLIP variant shows that the former component remains crucial for avoiding forgetting under resource-constrained settings.

4.1.1 Cross-Datasets Continual Learning (CDCL)

To simulate real-world settings with long sequence of tasks and large distribution shifts, the CDCL setting [19] trains a model sequentially on ImageNet100 and CIFAR100 (*i.e.*, on 20 tasks), and evaluates it jointly on these. For a fair comparison with [19], we adopt the ViT-L/14 as our CLIP backbone and set the train/test batch size to 32. All other settings remain the same as in Sec. 4.1. Table 2 reports the last task accuracy of different methods. While all our variants improve the CDCL performances of their respective baselines, combining ours with AttriCLIP [19] leads to the most gains. This further suggests that our framework can reliably leverage the diverse nature of learned prompts to inherit their setting-specific advantages.

4.2 Ablation Studies

We provide a few ablations of the training pipeline for CLAP4CLIP below and leave more in App. C.

Influence of components. We ablate the importance of different components of CLAP4CLIP in Table 3. On top of the base CLIP model, we first train a probabilistic encoder. Adding the VGA module and the memory consolidation training stage helps us achieve more stable performances while countering forgetting. We then apply task-specific encoders which make the centroids of the class-specific latent variable more separable (see Fig. 4) thus improving the last task accuracy by 2.21%. Language-aware weight initialization and regularization help improve the last task accuracies by 0.78% and 0.23%, respectively. Weight initialization further helps us tackle the *stability gap* [57, 58] (see App. C.6 for more ablations on language-aware components).

Probabilistic vs Deterministic inference. To understand our probabilistic inference modules further, we examine their performance against the deterministic variant of ours (Ours w/o VI). Table 1 shows that our probabilistic variant consistently outperforms its deterministic counterpart. This emphasizes the advantages of considering uncertainty in finetuning. We further introspect the effects of the number of layers for the VGA and task encoder modules in our framework in App. C.3.

https://doi.org/10.52202/079017-4102

Time analyses. We compare the inference time per iteration for different methods. As shown in App. Table 19, our variants need more inference time than other finetuning methods for the performance gains. The increased time comes mainly from the VGA and from inferring the M latent variables.

Parameter analyses. The additional parameters in CLAP4CLIP come from the shared VGA module and the task-specific encoders. For a ViT-B/16 backbone of output dimension, $d = 512$ on CIFAR100, the VGA module contains 4,204,032 parameters. The mean and the std. dev. layers for 10 tasks have $d \times d$ parameters each, *i.e.,* $524,2880$ parameters. Hence, the CLAP4CLIP has 9.5 million extra parameters, which is negligible compared to the pre-trained CLIP with ≈ 150 million parameters. We report the parameter counts in Fig. 5.

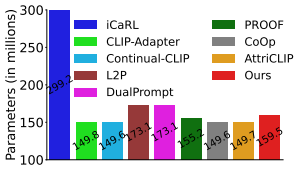

Figure 5: Parameter count comparison.

5 Out-of-the-box utilities of probabilistic finetuning

We study the out-of-the-box utilities of CLAP4CLIP's uncertainty quantification (UQ) capabilities. Our motivation for these is not to achieve state-of-the-art performance but to highlight the perks of probabilistic modeling in scenarios where the deterministic CL finetuning methods struggle.

Post-hoc novel data detection (PhNDD). PhNDD uses a pre-trained classification model to identify novel data based on the output confidence [71, 72]. For CL, this can help discern the arrival of new tasks, expand the network, etc. To evaluate the PhNDD capabilities of models within a CL setup, we design a simple setting. Namely, at all but the last test step, we treat the test data from the past and the current tasks as *seen* while those from all future tasks as *novel*. We then use FPR95, AUROC [73], and AUPR [74] scores as our performance metrics (see App. D.1) averaged over all but the last incremental test steps. To quantify the output confidence, we rely on the Energy score [75] given its aptness for pre-trained models. Table 4 compares the averaged PhNDD performances. Our probabilistic models enhance the PhNDD capabilities of their underlying prompting frameworks. Moreover, the inferior results of the deterministic (*i.e.*, w/o VI) versions of our models suggest that probabilistic modelling helps a model output predictions that better express what it is not aware of.

Method	AUROC ↑	AUPR ↑	FPR95 ↓
Continual-CLIP [14]	74.46	71.11	77.33
Ours w/o VI	**82.29**	78.88	68.83
Ours	82.21	**79.54**	**68.72**
CoOp [12]	80.15	77.62	66.8
+ Ours w/o VI	81.98	78.88	66.21
+ Ours	**83.73**	**80.97**	**62.68**

Table 4: PhNDD performances averaged over 3 runs on CIFAR100. Best scores for each variant are in **bold**.

Exemplar selection. We employ the entropy (averaged over M predictions) of CLAP's softmax outputs as our exemplar selection criteria [2]. Table 20 shows the efficacy of entropy-based rehearsal for our method, where other deterministic methods lag due to their inconsistent UQ capabilities. Next, we employ the energy [75] and the variance of the softmax outputs as our selection criterion and contrast these against other criteria proposed in [2]. Fig. 6 shows that variance-based exemplar selection outperforms random, and is only second to iCaRL [30] in terms of Last accuracy. We note that deterministic methods with pointwise predictions cannot use variance for exemplar selection.

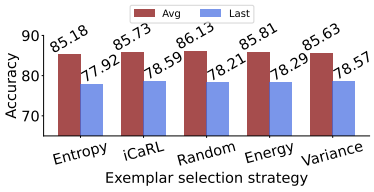

Figure 6: **Analyses of various strategies** for exemplar selection w/ our method on CIFAR100.

6 Conclusion

In this paper, we propose CLAP4CLIP, a probabilistic finetuning method for learning task-specific distributions over visual-guided textual features. Our model shares the visual-guided text alignment module across all tasks while adding lightweight task-specific encoders to learn fine-grained task distributions. Besides leading to little memory overhead, this architecture is compatible with several prompt-tuning-based methods thus helping us inherit their respective perks on different CL settings. Our experiments show the superior results of CLAP4CLIP across several datasets and settings. We conclude with two out-of-the-box utilities of our method wherein existing continual learning methods lag: post-hoc novel data detection and uncertainty-based exemplar selection. We discuss our limitations, potential future research directions, and the broader impact in App. sec. E.

7 Acknowledgement

This work was partially supported by a Discovery Early Career Researcher Award Fellowship (DE230101591) awarded by the Australian Research Council (ARC) to Dong Gong. We are grateful to Daniel Marczak and M. Jehanzeb Mirza for their insights on the need for continual finetuning of the pre-trained CLIP model.

References

[1] Alec Radford, Jong Wook Kim, Chris Hallacy, Aditya Ramesh, Gabriel Goh, Sandhini Agarwal, Girish Sastry, Amanda Askell, Pamela Mishkin, Jack Clark, et al. Learning transferable visual models from natural language supervision. In *International conference on machine learning*, pages 8748–8763. PMLR, 2021.

[2] Arslan Chaudhry, Puneet K Dokania, Thalaiyasingam Ajanthan, and Philip HS Torr. Riemannian walk for incremental learning: Understanding forgetting and intransigence. In *Proceedings of the European conference on computer vision (ECCV)*, pages 532–547, 2018.

[3] Friedemann Zenke, Ben Poole, and Surya Ganguli. Continual learning through synaptic intelligence. In *International conference on machine learning*, pages 3987–3995. PMLR, 2017.

[4] Saurav Jha, Martin Schiemer, Franco Zambonelli, and Juan Ye. Continual learning in sensor-based human activity recognition: An empirical benchmark analysis. *Information Sciences*, 575:1–21, 2021.

[5] Arslan Chaudhry, Marcus Rohrbach, Mohamed Elhoseiny, Thalaiyasingam Ajanthan, Puneet K Dokania, Philip HS Torr, and Marc'Aurelio Ranzato. On tiny episodic memories in continual learning. *arXiv preprint arXiv:1902.10486*, 2019.

[6] James Kirkpatrick, Razvan Pascanu, Neil Rabinowitz, Joel Veness, Guillaume Desjardins, Andrei A Rusu, Kieran Milan, John Quan, Tiago Ramalho, Agnieszka Grabska-Barwinska, et al. Overcoming catastrophic forgetting in neural networks. *Proceedings of the national academy of sciences*, 114(13):3521–3526, 2017.

[7] Marc Masana, Xialei Liu, Bartłomiej Twardowski, Mikel Menta, Andrew D Bagdanov, and Joost Van De Weijer. Class-incremental learning: survey and performance evaluation on image classification. *IEEE Transactions on Pattern Analysis and Machine Intelligence*, 45(5):5513–5533, 2022.

[8] Saurav Jha, Dong Gong, He Zhao, and Lina Yao. NPCL: Neural processes for uncertainty-aware continual learning. In *Thirty-seventh Conference on Neural Information Processing Systems*, 2023.

[9] Jean-Baptiste Alayrac, Jeff Donahue, Pauline Luc, Antoine Miech, Iain Barr, Yana Hasson, Karel Lenc, Arthur Mensch, Katherine Millican, Malcolm Reynolds, et al. Flamingo: a visual language model for few-shot learning. *Advances in Neural Information Processing Systems*, 35:23716–23736, 2022.

[10] Robin Rombach, Andreas Blattmann, Dominik Lorenz, Patrick Esser, and Björn Ommer. High-resolution image synthesis with latent diffusion models. In *Proceedings of the IEEE/CVF conference on computer vision and pattern recognition*, pages 10684–10695, 2022.

[11] Aaron van den Oord, Yazhe Li, and Oriol Vinyals. Representation learning with contrastive predictive coding. *arXiv preprint arXiv:1807.03748*, 2018.

[12] Kaiyang Zhou, Jingkang Yang, Chen Change Loy, and Ziwei Liu. Learning to prompt for vision-language models. *International Journal of Computer Vision*, 130(9):2337–2348, 2022.

[13] Peng Gao, Shijie Geng, Renrui Zhang, Teli Ma, Rongyao Fang, Yongfeng Zhang, Hongsheng Li, and Yu Qiao. Clip-adapter: Better vision-language models with feature adapters. *arXiv preprint arXiv:2110.04544*, 2021.

 https://doi.org/10.52202/079017-4102

[14] Vishal G. Thengane, Salman A. Khan, Munawar Hayat, and Fahad Shahbaz Khan. Clip model is an efficient continual learner. *ArXiv*, abs/2210.03114, 2022.

[15] Ananya Kumar, Aditi Raghunathan, Robbie Jones, Tengyu Ma, and Percy Liang. Fine-tuning can distort pretrained features and underperform out-of-distribution. *ICLR*, 2022.

[16] Yuning Lu, Jianzhuang Liu, Yonggang Zhang, Yajing Liu, and Xinmei Tian. Prompt distribution learning. In *Proceedings of the IEEE/CVF Conference on Computer Vision and Pattern Recognition*, pages 5206–5215, 2022.

[17] Mohammad Mahdi Derakhshani, Enrique Sanchez, Adrian Bulat, Victor G Turrisi da Costa, Cees GM Snoek, Georgios Tzimiropoulos, and Brais Martinez. Bayesian prompt learning for image-language model generalization. In *Proceedings of the IEEE/CVF International Conference on Computer Vision*, pages 15237–15246, 2023.

[18] Yann LeCun. A path towards autonomous machine intelligence version 0.9. 2, 2022-06-27. *Open Review*, 62, 2022.

[19] Runqi Wang, Xiaoyue Duan, Guoliang Kang, Jianzhuang Liu, Shaohui Lin, Songcen Xu, Jinhu Lü, and Baochang Zhang. Attriclip: A non-incremental learner for incremental knowledge learning. In *Proceedings of the IEEE/CVF Conference on Computer Vision and Pattern Recognition*, pages 3654–3663, 2023.

[20] Muhammad Uzair Khattak, Hanoona Rasheed, Muhammad Maaz, Salman Khan, and Fahad Shahbaz Khan. Maple: Multi-modal prompt learning. In *CVPR*, 2023.

[21] Yuji Iikubo, Shunsuke Horii, and Toshiyasu Matsushima. Model selection of bayesian hierarchical mixture of experts based on variational inference. In *2019 IEEE International Conference on Systems, Man and Cybernetics (SMC)*, pages 3474–3479, 2019.

[22] Oleksandr Balabanov, Bernhard Mehlig, and Hampus Linander. Bayesian posterior approximation with stochastic ensembles. In *2023 IEEE/CVF Conference on Computer Vision and Pattern Recognition (CVPR)*, pages 13701–13711. IEEE, 2023.

[23] Ameya Prabhu, Hasan Abed Al Kader Hammoud, Ser-Nam Lim, Bernard Ghanem, Philip HS Torr, and Adel Bibi. From categories to classifier: Name-only continual learning by exploring the web. *arXiv preprint arXiv:2311.11293*, 2023.

[24] Minhyuk Seo, Diganta Misra, Seongwon Cho, Minjae Lee, and Jonghyun Choi. Just say the name: Online continual learning with category names only via data generation. *arXiv preprint arXiv:2403.10853*, 2024.

[25] Rahaf Aljundi, Francesca Babiloni, Mohamed Elhoseiny, Marcus Rohrbach, and Tinne Tuytelaars. Memory aware synapses: Learning what (not) to forget. In *Proceedings of the European conference on computer vision (ECCV)*, pages 139–154, 2018.

[26] Saurav Jha, Shiqi Yang, Masato Ishii, Mengjie Zhao, Christian Simon, Muhammad Jehanzeb Mirza, Dong Gong, Lina Yao, Shusuke Takahashi, and Yuki Mitsufuji. Mining your own secrets: Diffusion classifier scores for continual personalization of text-to-image diffusion models. *arXiv preprint arXiv:2410.00700*, 2024.

[27] Arthur Douillard, Alexandre Ramé, Guillaume Couairon, and Matthieu Cord. Dytox: Transformers for continual learning with dynamic token expansion. In *Proceedings of the IEEE/CVF Conference on Computer Vision and Pattern Recognition*, pages 9285–9295, 2022.

[28] Oleksiy Ostapenko, Pau Rodriguez, Massimo Caccia, and Laurent Charlin. Continual learning via local module composition. *Advances in Neural Information Processing Systems*, 34:30298–30312, 2021.

[29] Haeyong Kang, Rusty John Lloyd Mina, Sultan Rizky Hikmawan Madjid, Jaehong Yoon, Mark Hasegawa-Johnson, Sung Ju Hwang, and Chang D Yoo. Forget-free continual learning with winning subnetworks. In *International Conference on Machine Learning*, pages 10734–10750. PMLR, 2022.

[30] Sylvestre-Alvise Rebuffi, Alexander Kolesnikov, Georg Sperl, and Christoph H Lampert. icarl: Incremental classifier and representation learning. In *Proceedings of the IEEE conference on Computer Vision and Pattern Recognition*, pages 2001–2010, 2017.

[31] Timothee LESORT and Andrei Stoian. Regularization shortcomings for continual learning, 2021.

[32] Eli Verwimp, Matthias De Lange, and Tinne Tuytelaars. Rehearsal revealed: The limits and merits of revisiting samples in continual learning. In *Proceedings of the IEEE/CVF International Conference on Computer Vision*, pages 9385–9394, 2021.

[33] Jiahui Yu, Zirui Wang, Vijay Vasudevan, Legg Yeung, Mojtaba Seyedhosseini, and Yonghui Wu. Coca: Contrastive captioners are image-text foundation models. *Transactions on Machine Learning Research*, 2022.

[34] Mitchell Wortsman, Gabriel Ilharco, Jong Wook Kim, Mike Li, Simon Kornblith, Rebecca Roelofs, Raphael Gontijo Lopes, Hannaneh Hajishirzi, Ali Farhadi, Hongseok Namkoong, et al. Robust fine-tuning of zero-shot models. In *Proceedings of the IEEE/CVF Conference on Computer Vision and Pattern Recognition*, pages 7959–7971, 2022.

[35] Hieu Pham, Zihang Dai, Golnaz Ghiasi, Kenji Kawaguchi, Hanxiao Liu, Adams Wei Yu, Jiahui Yu, Yi-Ting Chen, Minh-Thang Luong, Yonghui Wu, et al. Combined scaling for zero-shot transfer learning. *Neurocomputing*, page 126658, 2023.

[36] Renrui Zhang, Wei Zhang, Rongyao Fang, Peng Gao, Kunchang Li, Jifeng Dai, Yu Qiao, and Hongsheng Li. Tip-adapter: Training-free adaption of clip for few-shot classification. In *European Conference on Computer Vision*, pages 493–510. Springer, 2022.

[37] Kaiyang Zhou, Jingkang Yang, Chen Change Loy, and Ziwei Liu. Conditional prompt learning for vision-language models. In *Proceedings of the IEEE/CVF Conference on Computer Vision and Pattern Recognition*, pages 16816–16825, 2022.

[38] James Seale Smith, Leonid Karlinsky, Vyshnavi Gutta, Paola Cascante-Bonilla, Donghyun Kim, Assaf Arbelle, Rameswar Panda, Rogerio Feris, and Zsolt Kira. Coda-prompt: Continual decomposed attention-based prompting for rehearsal-free continual learning. In *Proceedings of the IEEE/CVF Conference on Computer Vision and Pattern Recognition*, pages 11909–11919, 2023.

[39] Da-Wei Zhou, Yuanhan Zhang, Jingyi Ning, Han-Jia Ye, De-Chuan Zhan, and Ziwei Liu. Learning without forgetting for vision-language models. *arXiv preprint arXiv:2305.19270*, 2023.

[40] Zhizhong Li and Derek Hoiem. Learning without forgetting. *IEEE transactions on pattern analysis and machine intelligence*, 40(12):2935–2947, 2017.

[41] Saihui Hou, Xinyu Pan, Chen Change Loy, Zilei Wang, and Dahua Lin. Learning a unified classifier incrementally via rebalancing. In *Proceedings of the IEEE/CVF conference on computer vision and pattern recognition*, pages 831–839, 2019.

[42] Francisco M Castro, Manuel J Marín-Jiménez, Nicolás Guil, Cordelia Schmid, and Karteek Alahari. End-to-end incremental learning. In *Proceedings of the European conference on computer vision (ECCV)*, pages 233–248, 2018.

[43] Yue Wu, Yinpeng Chen, Lijuan Wang, Yuancheng Ye, Zicheng Liu, Yandong Guo, and Yun Fu. Large scale incremental learning. In *Proceedings of the IEEE/CVF conference on computer vision and pattern recognition*, pages 374–382, 2019.

[44] Max Welling. Herding dynamical weights to learn. In *Proceedings of the 26th Annual International Conference on Machine Learning*, pages 1121–1128, 2009.

[45] Diederik P Kingma and Max Welling. Auto-encoding variational bayes. *arXiv preprint arXiv:1312.6114*, 2013.

 https://doi.org/10.52202/079017-4102

[46] Yuchao Gu, Xintao Wang, Jay Zhangjie Wu, Yujun Shi, Yunpeng Chen, Zihan Fan, Wuyou Xiao, Rui Zhao, Shuning Chang, Weijia Wu, et al. Mix-of-show: Decentralized low-rank adaptation for multi-concept customization of diffusion models. *Advances in Neural Information Processing Systems*, 36, 2024.

[47] Zixuan Ni, Longhui Wei, Siliang Tang, Yueting Zhuang, and Qi Tian. Continual vision-language representaion learning with off-diagonal information, 2023.

[48] Ashish Vaswani, Noam Shazeer, Niki Parmar, Jakob Uszkoreit, Llion Jones, Aidan N Gomez, Łukasz Kaiser, and Illia Polosukhin. Attention is all you need. *Advances in neural information processing systems*, 30, 2017.

[49] Longtian Qiu, Renrui Zhang, Ziyu Guo, Ziyao Zeng, Yafeng Li, and Guangnan Zhang. Vt-clip: Enhancing vision-language models with visual-guided texts. *arXiv preprint arXiv:2112.02399*, 2021.

[50] Alexey Dosovitskiy, Lucas Beyer, Alexander Kolesnikov, Dirk Weissenborn, Xiaohua Zhai, Thomas Unterthiner, Mostafa Dehghani, Matthias Minderer, Georg Heigold, Sylvain Gelly, Jakob Uszkoreit, and Neil Houlsby. An image is worth 16x16 words: Transformers for image recognition at scale. In *International Conference on Learning Representations*, 2021.

[51] Stanislav Fort, Huiyi Hu, and Balaji Lakshminarayanan. Deep ensembles: A loss landscape perspective. *arXiv preprint arXiv:1912.02757*, 2019.

[52] Shipeng Yan, Jiangwei Xie, and Xuming He. Der: Dynamically expandable representation for class incremental learning. In *Proceedings of the IEEE/CVF Conference on Computer Vision and Pattern Recognition*, pages 3014–3023, 2021.

[53] Alec Radford, Karthik Narasimhan, Tim Salimans, Ilya Sutskever, et al. Improving language understanding by generative pre-training. 2018.

[54] Dongyue Li and Hongyang Zhang. Improved regularization and robustness for fine-tuning in neural networks. In A. Beygelzimer, Y. Dauphin, P. Liang, and J. Wortman Vaughan, editors, *Advances in Neural Information Processing Systems*, 2021.

[55] Pingbo Pan, Siddharth Swaroop, Alexander Immer, Runa Eschenhagen, Richard Turner, and Mohammad Emtiyaz E Khan. Continual deep learning by functional regularisation of memorable past. In H. Larochelle, M. Ranzato, R. Hadsell, M.F. Balcan, and H. Lin, editors, *Advances in Neural Information Processing Systems*, volume 33, pages 4453–4464. Curran Associates, Inc., 2020.

[56] Adrian Bulat and Georgios Tzimiropoulos. Language-aware soft prompting for vision & language foundation models, 2023.

[57] Matthias De Lange, Gido M van de Ven, and Tinne Tuytelaars. Continual evaluation for lifelong learning: Identifying the stability gap. In *The Eleventh International Conference on Learning Representations*, 2023.

[58] Md Yousuf Harun and Christopher Kanan. Overcoming the stability gap in continual learning. *arXiv preprint arXiv:2306.01904*, 2023.

[59] Zifeng Wang, Zizhao Zhang, Sayna Ebrahimi, Ruoxi Sun, Han Zhang, Chen-Yu Lee, Xiaoqi Ren, Guolong Su, Vincent Perot, Jennifer Dy, et al. Dualprompt: Complementary prompting for rehearsal-free continual learning. In *European Conference on Computer Vision*, pages 631–648. Springer, 2022.

[60] Catherine Wah, Steve Branson, Peter Welinder, Pietro Perona, and Serge Belongie. The caltech-ucsd birds-200-2011 dataset. 2011.

[61] Alex Krizhevsky. Learning multiple layers of features from tiny images. 2009.

[62] Alex Krizhevsky, Ilya Sutskever, and Geoffrey E Hinton. Imagenet classification with deep convolutional neural networks. *Advances in neural information processing systems*, 25, 2012.

[63] Dan Hendrycks, Steven Basart, Norman Mu, Saurav Kadavath, Frank Wang, Evan Dorundo, Rahul Desai, Tyler Zhu, Samyak Parajuli, Mike Guo, et al. The many faces of robustness: A critical analysis of out-of-distribution generalization. In *Proceedings of the IEEE/CVF International Conference on Computer Vision*, pages 8340–8349, 2021.

[64] Da-Wei Zhou, Han-Jia Ye, De-Chuan Zhan, and Ziwei Liu. Revisiting class-incremental learning with pre-trained models: Generalizability and adaptivity are all you need. *arXiv preprint arXiv:2303.07338*, 2023.

[65] Zifeng Wang, Zizhao Zhang, Chen-Yu Lee, Han Zhang, Ruoxi Sun, Xiaoqi Ren, Guolong Su, Vincent Perot, Jennifer Dy, and Tomas Pfister. Learning to prompt for continual learning. In *Proceedings of the IEEE/CVF Conference on Computer Vision and Pattern Recognition*, pages 139–149, 2022.

[66] David Lopez-Paz and Marc'Aurelio Ranzato. Gradient episodic memory for continual learning. *Advances in neural information processing systems*, 30, 2017.

[67] Mahdi Pakdaman Naeini, Gregory F. Cooper, and Milos Hauskrecht. Obtaining well calibrated probabilities using bayesian binning. *Proceedings of the ... AAAI Conference on Artificial Intelligence. AAAI Conference on Artificial Intelligence*, 2015:2901–2907, 2015.

[68] Matthias Minderer, Josip Djolonga, Rob Romijnders, Frances Hubis, Xiaohua Zhai, Neil Houlsby, Dustin Tran, and Mario Lucic. Revisiting the calibration of modern neural networks. *Advances in Neural Information Processing Systems*, 34:15682–15694, 2021.

[69] Zangwei Zheng, Mingyuan Ma, Kai Wang, Ziheng Qin, Xiangyu Yue, and Yang You. Preventing zero-shot transfer degradation in continual learning of vision-language models. In *ICCV*, October 2023.

[70] Francesco Pelosin, Saurav Jha, Andrea Torsello, Bogdan Raducanu, and Joost van de Weijer. Towards exemplar-free continual learning in vision transformers: An account of attention, functional and weight regularization. In *Proceedings of the IEEE/CVF Conference on Computer Vision and Pattern Recognition (CVPR) Workshops*, pages 3820–3829, June 2022.

[71] Jingkang Yang, Kaiyang Zhou, Yixuan Li, and Ziwei Liu. Generalized out-of-distribution detection: A survey. *arXiv preprint arXiv:2110.11334*, 2021.

[72] Jiangpeng He and Fengqing Zhu. Out-of-distribution detection in unsupervised continual learning. In *Proceedings of the IEEE/CVF Conference on Computer Vision and Pattern Recognition*, pages 3850–3855, 2022.

[73] Jesse Davis and Mark Goadrich. The relationship between precision-recall and roc curves. In *Proceedings of the 23rd international conference on Machine learning*, pages 233–240, 2006.

[74] Takaya Saito and Marc Rehmsmeier. The precision-recall plot is more informative than the roc plot when evaluating binary classifiers on imbalanced datasets. *PloS one*, 10(3):e0118432, 2015.

[75] Weitang Liu, Xiaoyun Wang, John Owens, and Yixuan Li. Energy-based out-of-distribution detection. *Advances in neural information processing systems*, 33:21464–21475, 2020.

[76] Xiaohua Zhai, Joan Puigcerver, Alexander Kolesnikov, Pierre Ruyssen, Carlos Riquelme, Mario Lucic, Josip Djolonga, Andre Susano Pinto, Maxim Neumann, Alexey Dosovitskiy, et al. A large-scale study of representation learning with the visual task adaptation benchmark. *arXiv preprint arXiv:1910.04867*, 2019.

[77] Gong Cheng, Junwei Han, and Xiaoqiang Lu. Remote sensing image scene classification: Benchmark and state of the art. *Proceedings of the IEEE*, 105(10):1865–1883, 2017.

[78] Mircea Cimpoi, Subhransu Maji, Iasonas Kokkinos, Sammy Mohamed, and Andrea Vedaldi. Describing textures in the wild. In *Proceedings of the IEEE conference on computer vision and pattern recognition*, pages 3606–3613, 2014.

 https://doi.org/10.52202/079017-4102

[79] Omkar M Parkhi, Andrea Vedaldi, Andrew Zisserman, and C. V. Jawahar. Cats and dogs. In *2012 IEEE Conference on Computer Vision and Pattern Recognition*, pages 3498–3505, 2012.

[80] Patrick Helber, Benjamin Bischke, Andreas Dengel, and Damian Borth. Eurosat: A novel dataset and deep learning benchmark for land use and land cover classification. *IEEE Journal of Selected Topics in Applied Earth Observations and Remote Sensing*, 12(7):2217–2226, 2019.

[81] M-E Nilsback and Andrew Zisserman. A visual vocabulary for flower classification. In *2006 IEEE computer society conference on computer vision and pattern recognition (CVPR'06)*, volume 2, pages 1447–1454. IEEE, 2006.

[82] Da-Wei Zhou, Qi-Wei Wang, Zhi-Hong Qi, Han-Jia Ye, De-Chuan Zhan, and Ziwei Liu. Deep class-incremental learning: A survey. *arXiv preprint arXiv:2302.03648*, 2023.

[83] Sebastian Farquhar and Yarin Gal. Towards robust evaluations of continual learning. *International Conference on Machine Learning (ICML) Workshop*, page 9, 2018.

[84] Z. Zheng, M. Ma, K. Wang, Z. Qin, X. Yue, and Y. You. Preventing zero-shot transfer degradation in continual learning of vision-language models. In *2023 IEEE/CVF International Conference on Computer Vision (ICCV)*, pages 19068–19079, Los Alamitos, CA, USA, oct 2023. IEEE Computer Society.

[85] Edward J Hu, yelong shen, Phillip Wallis, Zeyuan Allen-Zhu, Yuanzhi Li, Shean Wang, Lu Wang, and Weizhu Chen. LoRA: Low-rank adaptation of large language models. In *International Conference on Learning Representations*, 2022.

[86] Youngjae Cho, HeeSun Bae, Seungjae Shin, Yeo Dong Youn, Weonyoung Joo, and Il-Chul Moon. Make prompts adaptable: Bayesian modeling for vision-language prompt learning with data-dependent prior. *arXiv preprint arXiv:2401.06799*, 2024.

[87] Tejas Srinivasan, Ting-Yun Chang, Leticia Pinto Alva, Georgios Chochlakis, Mohammad Rostami, and Jesse Thomason. Climb: A continual learning benchmark for vision-and-language tasks. *Advances in Neural Information Processing Systems*, 35:29440–29453, 2022.

[88] Zifeng Wang, Zheng Zhan, Yifan Gong, Geng Yuan, Wei Niu, Tong Jian, Bin Ren, Stratis Ioannidis, Yanzhi Wang, and Jennifer Dy. Sparcl: Sparse continual learning on the edge. *Advances in Neural Information Processing Systems*, 35:20366–20380, 2022.

[89] Qingsen Yan, Dong Gong, Yuhang Liu, Anton van den Hengel, and Javen Qinfeng Shi. Learning bayesian sparse networks with full experience replay for continual learning. In *Proceedings of the IEEE/CVF Conference on Computer Vision and Pattern Recognition*, pages 109–118, 2022.

[90] Sachit Menon and Carl Vondrick. Visual classification via description from large language models. In *The Eleventh International Conference on Learning Representations*, 2023.

[91] Sarah Pratt, Ian Covert, Rosanne Liu, and Ali Farhadi. What does a platypus look like? generating customized prompts for zero-shot image classification. In *Proceedings of the IEEE/CVF International Conference on Computer Vision*, pages 15691–15701, 2023.

[92] Muhammad Uzair Khattak, Muhammad Ferjad Naeem, Muzammal Naseer, Luc Van Gool, and Federico Tombari. Learning to prompt with text only supervision for vision-language models. *arXiv preprint arXiv:2401.02418*, 2024.

[93] Tom Brown, Benjamin Mann, Nick Ryder, Melanie Subbiah, Jared D Kaplan, Prafulla Dhariwal, Arvind Neelakantan, Pranav Shyam, Girish Sastry, Amanda Askell, et al. Language models are few-shot learners. *Advances in neural information processing systems*, 33:1877–1901, 2020.

[94] Tejas Srinivasan, Furong Jia, Mohammad Rostami, and Jesse Thomason. I2i: Initializing adapters with improvised knowledge. *arXiv preprint arXiv:2304.02168*, 2023.

[95] Mike Lewis, Yinhan Liu, Naman Goyal, Marjan Ghazvininejad, Abdelrahman Mohamed, Omer Levy, Veselin Stoyanov, and Luke Zettlemoyer. Bart: Denoising sequence-to-sequence pre-training for natural language generation, translation, and comprehension. In *Proceedings of the 58th Annual Meeting of the Association for Computational Linguistics*, pages 7871–7880, 2020.

[96] Jonathan Ho and Tim Salimans. Classifier-free diffusion guidance. *arXiv preprint arXiv:2207.12598*, 2022.

[97] Rinon Gal, Yuval Alaluf, Yuval Atzmon, Or Patashnik, Amit H Bermano, Gal Chechik, and Daniel Cohen-Or. An image is worth one word: Personalizing text-to-image generation using textual inversion. *arXiv preprint arXiv:2208.01618*, 2022.

[98] James Seale Smith, Yen-Chang Hsu, Lingyu Zhang, Ting Hua, Zsolt Kira, Yilin Shen, and Hongxia Jin. Continual diffusion: Continual customization of text-to-image diffusion with c-lora. *arXiv preprint arXiv:2304.06027*, 2023.

[99] Vincent Fortuin. Priors in bayesian deep learning: A review. *International Statistical Review*, 90(3):563–591, 2022.

[100] Andrew Gelman. Prior distributions for variance parameters in hierarchical models (comment on article by browne and draper). *Bayesian Analysis*, 1:515–534, 2004.

[101] Bernt Øksendal and Bernt Øksendal. *Stochastic differential equations*. Springer, 2003.

[102] Marta Garnelo, Jonathan Schwarz, Dan Rosenbaum, Fabio Viola, Danilo J Rezende, SM Eslami, and Yee Whye Teh. Neural processes. *arXiv preprint arXiv:1807.01622*, 2018.

[103] Donggyun Kim, Seongwoong Cho, Wonkwang Lee, and Seunghoon Hong. Multi-task processes. In *International Conference on Learning Representations*, 2022.

[104] Tuan Anh Le, Hyunjik Kim, Marta Garnelo, Dan Rosenbaum, Jonathan Schwarz, and Yee Whye Teh. Empirical evaluation of neural process objectives. In *NeurIPS workshop on Bayesian Deep Learning*, volume 4, 2018.

 https://doi.org/10.52202/079017-4102

Appendix

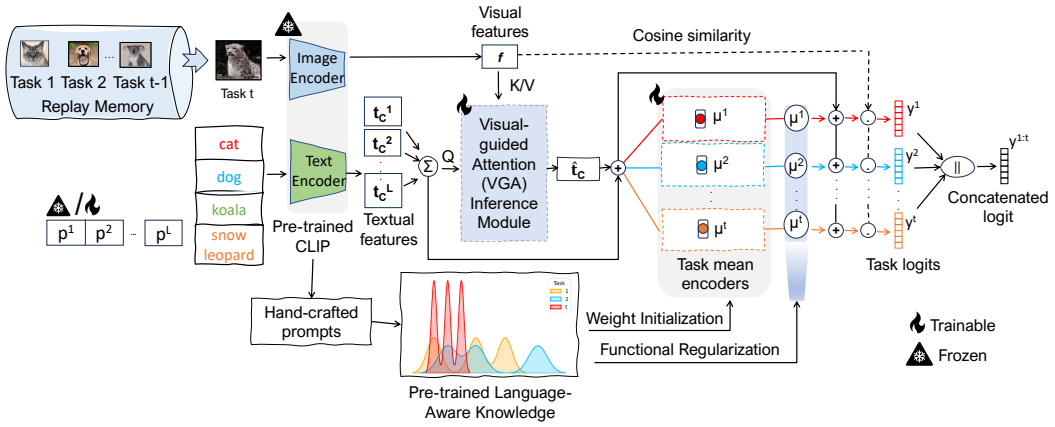

Figure 7: **Illustration of the deterministic variant of Ours (Ours w/o VI in Table 1):** the task-specific text features are fed to their respective task encoders, consisting of only the mean μ layer each. There is no sampling involved and the task mean outputs are fused directly with the original task features prior to deriving the task logits $\mathbf{y}^t$. All task logits are concatenated to produce the final prediction $\mathbf{y}^{1:t}$.

A Experiments and Benchmarks

A.1 Datasets

Dataset	# training instances	# testing instances	# Classes	# Tasks	Link
CIFAR100	50,000	10,000	100	10	URL
ImageNet100	130,000	5,000	100	10	URL
ImageNet-R	24,000	6,000	200	10	URL
CUB200	9,430	2,358	200	10	URL
VTAB	1,796	8,619	50	5	URL

Table 5: **Benchmark datasets** and their details.

We evaluate our method on five datasets, the details of which are reported in Table 5. Following [39], we shuffle the order of training classes for all but the VTAB dataset with the random seed 1993. While the original VTAB [76] includes 19 evaluation tasks from three categories (*natural*, *specialized*, and *structured*) and their respective sub-domains, we rely on the five datasets cross-domain class-incremental subset proposed in SimpleCIL [64]. The five datasets (used in the same streaming order) include Resisc45 [77], DTD [78], Pets [79], EuroSAT [80], and Flowers [81]. To make the classes emerge from domain to domain, we do not shuffle the class order for VTAB.

A.1.1 Exemplar selection for memory replay

Following [30, 41], we employ the herding algorithm [44] to choose the exemplars for our main experiments. Following the previous works [82, 39], we rely on two typical methods to populate the memory:

1. **Fixed memory budget** maintains a static memory $\mathcal{M}$ with K instances. Upon having seen $|\mathcal{Y}_b|$ number of classes after an incremental training stage, the model selects $\frac{K}{|\mathcal{Y}_b|}$ exemplars per class.

https://doi.org/10.52202/079017-4102

2. **Expandable exemplar set** dynamically expands the memory $\mathcal{M}$ with the arrival of more incremental tasks. After each incremental training stage, the model here stores $|\mathcal{Y}_b| \times k_c$ exemplars, where k_c is the number of exemplars per class.

For CIFAR100, ImageNet100, and VTAB, given their lesser number of classes, we employ the first policy, and keep a total of 2,000, 1,000, and 1,000 exemplars, respectively. This amounts to the respective sub-totals of 20 and 10 exemplars per class after the last incremental stage. We choose these sizes for a straightforward comparison with the existing works, *i.e.,* PROOF [39] for CIFAR100 and AttriCLIP [19] for ImageNet100. For VTAB, the chosen memory size reflects the fact that we have only $1,796$ training instances in total (see Table 5). For ImageNet-R and CUB200 with 200 classes each, we adopt the second policy and store 20 exemplars per class.

A.2 Training and Hyperparameter selection

We train CLAP and its variants using SGD, with a batch size of 64, for 5 epochs, including 1 epoch of linear warmup. The initial learning rate (LR) is set to 1e-3 and decays with cosine annealing. At the end of each incremental task ($t > 1$), we perform memory consolidation training for 2 epochs, with an LR of 1e-4, on the class-balanced memory dataset. All our experiments were performed on NVIDIA V100 GPUs hosted on the Gadi supercomputers of the National Computational Infrastructure (NCI Australia).

Training for memory consolidation. To alleviate the forgetting of past tasks, we finetune on the class-balanced dataset of new data and rehearsal data $\mathcal{M}$ at the end of each incremental training step ($t > 1$) [41, 27]. Following other well-established parameter-isolation CL algorithms [27, 42, 52], we freeze the past task encoders during the normal training. This helps us avoid knowledge interference from the dominant new task training samples. During the memory consolidation training stage, we optimize all the task encoders while freezing the task-shared VGA module parameters.

Hyperparameter tuning. To the end goal of obtaining task-agnostic hyperparameters [83], we tuned our hyperparameters using a validation set comprising 10% of the CIFAR-100 training dataset. Similar to [27], performing the hyperparameter search only on the CIFAR100 setup helps us avoid optimizing for the number of tasks while generalizing across all our other setups. Table 6 shows the candidate values for the hyperparameter grid search and their best-chosen values. Tables 7, 8, 9, and 10 report the last task accuracy scores (Last) corresponding to the hyperparameter search for the number of training epochs, the number of finetuning epochs, the coefficient γ and the coefficient λ, respectively. Fig. 9 in the main paper reports the accuracy and the runtimes for the different numbers of MC samples M. *We will release the full source code upon the acceptance of our paper.*

Hyperparameter	Range	Chosen value
Learning rate	$5e$-3, $1e$-3, $5e$-4	$1e$-3
Epochs	$3, 5, 7$	5
Warmup epochs	$0.5, 1, 1.5$	1
Finetuning epochs	$1, 2, 3, 4$	2
γ	$1, 5, 10, 15, 20, 25$	15
λ	$0.0001, 0.001, 0.01, 0.1$	0.001
M	$1, 5, 10, 15, 20, 25, 30, 50$	20

Table 6: **Hyperparameter tuning**: we run a gridsearch on the CIFAR100 setup with a validation set comprising 10% of the training set. The chosen values are reused across all other setups.

Epochs	3	5	7
Last	77.32	78.21	78.18

Table 7: Accuracy vs. Training epochs

Finetuning ep.	1	2	3	4
Last	77.65	78.21	78.2	78.18

Table 8: Accuracy vs. Finetuning epochs

https://doi.org/10.52202/079017-4102

γ	1	5	10	15	20	25
Last	78.04	77.94	78.1	78.21	77.96	77.14

Table 9: Accuracy vs. weight "γ" for $\mathcal{L}_{\text{KD}}$

λ	0.0001	0.001	0.01	0.1
Last	78.16	78.21	77.99	77.4

Table 10: Accuracy vs. weight "λ" for $\mathbb{D}_{\text{KL}}$

A.3 Variational modeling of text feature space vs. image feature space

We opt for the probabilistic modeling of task-specific text feature space rather than the image feature space mainly in light of the practical constraints imposed by the class-incremental learning (CIL) setting. In CIL, at test time, we are not given the task labels for images. As such, if we were to use task-specific adapters to model task-specific visual features distribution (rather than task-specific text features distribution), then we must infer which images are to be routed to what adapter. Existing solutions [8] to task id inference would route the text-guided visual features to all available adapters and then infer the correct prediction based on the adapter's outputs. Such an exhaustive routing mechanism greatly increases the test-time computational burden. Instead, we exploit the multimodal nature of CLIP [1] to model the distribution of visual-guided text features. This helps us avoid test-time task id inference as now our visual features form a shared context to which all task-specific text features (which we can distinguish simply by their labels) can attend. By sampling from the distributions over such visual-guided task-specific text features, we compute their cosine similarities with the visual features to obtain our predictive logits.

A.4 Latency comparison for VT-CLIP styled VGA vs Ours

We compare the performance of VT-CLIP-styled VGA with Ours. To align the text features with the image features, the former uses per-pixel spatial features obtained from the ViT prior to global pooling while we use the globally pooled features. Table 11 shows that VT-CLIP styled VGA achieves similar accuracy as ours while incurring $\approx 6\times$ higher inference time.

Method	**Avg.**	**Last**	**Inference time (s)**
VT-CLIP styled VGA	**86.54**	77.98	0.94
Ours	86.13	**78.21**	**0.16**

Table 11: Performance comparison of VT-CLIP styled VGA with Ours on CIFAR-100.

A.5 Algorithm overview.

B Results

B.1 Performance evolution

To complement the results in Table 1, Fig. 8 compares the accuracy of different methods at each evaluation step across all datasets. Our major conclusions are briefed as follows. A) The base task performance of CLAP4CLIP (ours) is consistently higher than other methods including the state-of-the-art PROOF [39]. This suggests that our probabilistic finetuning framework is effective for general downstream tasks in a non-incremental setting. B) For the CL settings in Table 1 where either of the CLAP4CLIP variants achieve the best performances, their performance curves also consistently retain superior results across all evaluation steps. This validates the effectiveness of our method at tackling forgetting. C) Similar to [39], we notice that CLAP4CLIP achieves a significant performance improvement over vision-only methods (L2P and DualPrompt). This indicates the merits of considering text and visual cues together for continual learning.

Algorithm 1: A forward CLAP4CLIP pass at test step t

Input : $\{\mathbf{t}^i\}_{i=1}^t$: text features, $f(x)$: image features
Output : $\hat{y}^{1:t}$ (predictions for classes seen till task t)

$\{\hat{\mathbf{t}}^i\}_{i=1}^t \leftarrow \text{VGA}(\{\mathbf{t}^i\}_{i=1}^t, f(x))$ // Eq. (5a)
for $i \leftarrow 1;\ i \leq t;\ i \mathrel{+}= 1$ **do**
  $\tilde{\mathbf{t}}^i = \hat{\mathbf{t}}^i + \mathbf{t}^i$ // Eq. (5b)
  $\mathcal{N}(\mu^i, \sigma^i) \leftarrow q_\phi^i(\tilde{\mathbf{t}}_c^i)$ // Sec. 3.2.3
  $\hat{y}^i \leftarrow \emptyset$ // Null prediction set
  for $m \leftarrow 1;\ m \leq M;\ m \mathrel{+}= 1$ **do**
    $z_m^i \sim \mathcal{N}(\mu^i, \sigma^i)$ // Sampling
    $\tilde{\mathbf{t}}_m^i \leftarrow \tilde{\mathbf{t}}^i + z_m^i$ // Fusion
    $\hat{y}_m^i \leftarrow \langle f(\mathbf{x})^T, \tilde{\mathbf{t}}_m^i \rangle$ // Using Eq. (3b)
    $\hat{y}^i \leftarrow \hat{y}^i \cup \hat{y}_m^i$ // Set Union
$\hat{y}^{1:t} \leftarrow [\hat{y}^1, ..., \hat{y}^t]$ // Concatenation

Method	CIFAR100	ImageNet100	ImageNet-R	CUB	VTAB
Continual-CLIP [14]	1.416	2.175	1.98	2.087	0.614
+Ours	1.39	2.19	1.86	2.06	0.443
CoOp [12]	1.57	2.47	1.95	1.99	0.54
+Ours	1.533	2.074	2.011	1.885	0.516
MaPLe [20]	1.3	2.052	2.16	1.803	0.49
+Ours	1.36	1.956	1.84	1.62	0.407
AttriCLIP [19]	1.781	2.54	2.37	2.419	0.996
+Ours	1.677	2.019	2.388	2.410	0.98

Table 12: **Standard deviation** (std. dev.) scores comparison for Avg. accuracy scores of Table 1 between our variants and their corresponding baseline prompt-based finetuning methods over three runs. In general, our std. dev. scores are comparable to or lower than the corresponding baseline methods and are thus statistically significant.

Method	CIFAR100	ImageNet100	ImageNet-R	CUB	VTAB
Continual-CLIP [14]	**-0.086**	**-0.091**	**-0.066**	-0.124	-0.041
+Ours	-0.106	-0.117	-0.107	**-0.117**	**0.012**
CoOp [12]	-0.257	-0.338	-0.12	-0.162	-0.007
+Ours	**-0.129**	**-0.139**	**-0.112**	**-0.106**	**0.011**
MaPLe [20]	-0.209	-0.352	-0.1	-0.145	**0.037**
+Ours	**-0.105**	**-0.112**	**-0.093**	**-0.102**	0.005
AttriCLIP [19]	**-0.128**	-0.152	**-0.082**	-0.151	-0.099
+Ours	-0.143	**-0.1**	-0.092	**-0.037**	**0.041**

Table 13: **Backward Transfer** (BwT) scores ↑ comparison between our variants and their corresponding baseline prompt-based finetuning methods averaged over three runs. Best scores across each pair is highlighted in **bold**.

Method	CIFAR100	ImageNet100	ImageNet-R	CUB	VTAB
Continual-CLIP [14]	65.34	**53.13**	61.67	**59.55**	65.13
+Ours	**65.47**	53.07	**64.05**	58.11	**66.91**
CoOp [12]	64.09	52.6	60.93	**62.11**	69.38
+Ours	**66.2**	**55.09**	**63.44**	58.6	**74.1**
MaPLe [20]	68.22	57.04	66.56	61.6	71.51
+Ours	**76.17**	**62.33**	**70.03**	**67.8**	**78.29**
AttriCLIP [19]	61.45	50.4	56.41	57.04	61.59
+Ours	**61.87**	**50.56**	**58.03**	**57.95**	**64.3**

Table 14: **Transfer** scores [84] ↑ comparison between our variants and their corresponding baseline prompt-based finetuning methods averaged over three runs. Best scores across each pair is highlighted in **bold**.

https://doi.org/10.52202/079017-4102

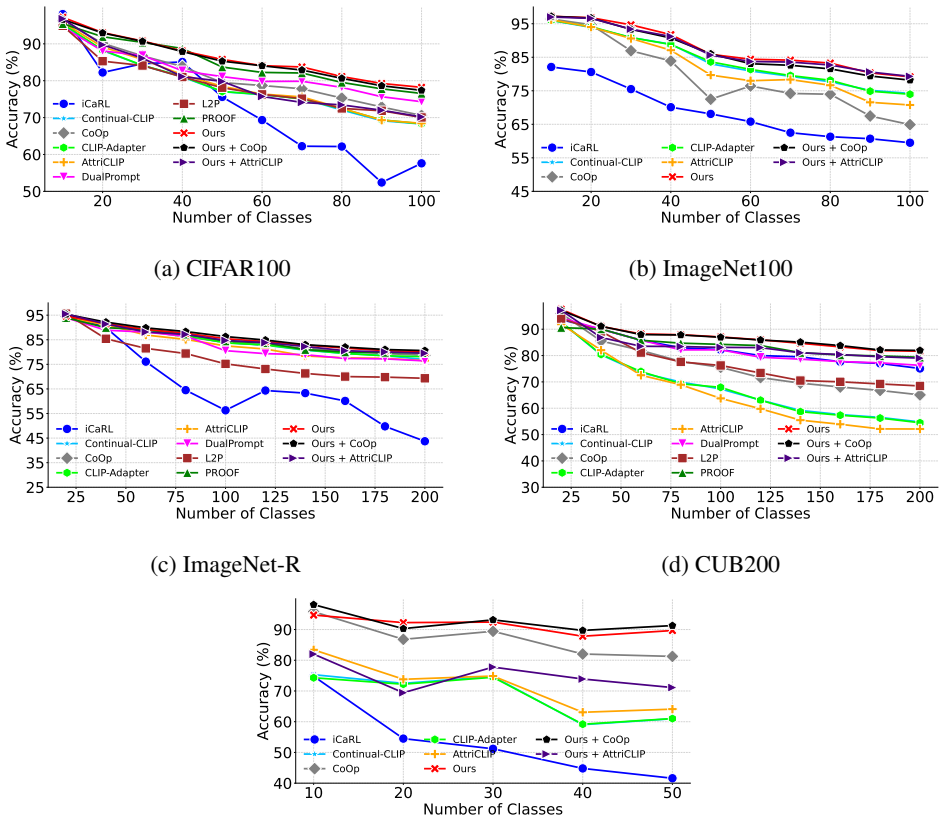

(a) CIFAR100

(b) ImageNet100

(c) ImageNet-R

(d) CUB200

(e) VTAB

Figure 8: **Performance evolution of different methods.** The top-1 accuracy (%) is reported upon learning of each task.

Method	CIFAR100	ImageNet100	ImageNet-R	CUB	VTAB
Continual-CLIP [14]	0.288	0.238	0.206	0.208	0.186
+Ours	**0.216**	**0.207**	**0.201**	**0.203**	**0.165**
CoOp [12]	0.245	0.3	**0.191**	0.21	0.191
+Ours	**0.224**	**0.217**	0.207	**0.204**	**0.136**
MaPLe [20]	**0.168**	0.243	0.149	0.195	0.195
+Ours	0.214	**0.208**	**0.146**	**0.184**	**0.159**
AttriCLIP [19]	**0.256**	0.256	0.205	0.209	**0.191**
+Ours	0.304	**0.205**	**0.19**	**0.198**	0.304

Table 15: **Expected Calibration Error** (ECE) scores ↓ (computed over 15 bins) comparison between our variants and their corresponding baseline prompt-based finetuning methods averaged over three runs. Best scores across each pair is highlighted in **bold**.

B.2 Results for replay-free CL setup

Method	CIFAR100		ImageNet100		ImageNet-R		CUB200		VTAB	
	Avg ↑	**Last** ↑	**Avg** ↑	**Last** ↑	**Avg** ↑	**Last** ↑	**Avg** ↑	**Last** ↑	**Avg** ↑	**Last** ↑
CODA-P	74.66	63.7	79.8	72.66	76.44	72.19	74.32	70.15	70.59	66.12
AttriCLIP [19]	71.35	61.4	80.55	73.08	79.57	76.1	73.89	72.36	71.25	66.02
CoOp + Ours	74.19	63.45	81.07	72.0	81.22	75.8	**82.59**	**74.98**	**82.11**	**80.11**
AttriCLIP + Ours	**76.94**	**69.39**	**84.1**	**75.83**	**85.2**	**78.57**	77.2	73.58	72.98	68.5
AttriCLIP + Ours (w/o adapter init)	71.87	60.35	75.9	69.41	77.1	70.53	69.82	65.95	65.48	61.35
AttriCLIP + Ours (w/o distribution reg.)	64.2	53.01	64.03	52.55	62.81	53.19	58.52	51.0	58.22	56.14

Table 16: **Performance comparison without memory replay** (avg. over 3 runs). For a thorough analysis, the last two rows ablate our proposed pretrained CLIP's language-aware anti-forgetting components (Sec. 3.3, main paper): distribution regularization and adapter weight initialization. Best results are in **bold**.

B.3 Results for computationally-budgeted CL setup

For our computationally-budgeted CL setup, we follow [23] where on each incremental training task, we allocate the number of training iterations equivalent to 1 epoch on the first (base) task of each dataset. Here, our variant utilizing instance-conditioned prompts of AttriCLIP outperforms other compared methods. A further ablation shows that our proposed weight distribution regularization technique indeed remains a crucial component at tackling forgetting on the budgeted setup (see the two bottom-most rows in Table 17).

Method	CIFAR100		ImageNet100	
	Avg ↑	**Last** ↑	**Avg** ↑	**Last** ↑
CODA-P	52.13	49.5	52.99	48.03
AttriCLIP [19]	58.61	52.1	60.54	57.4
PROOF	55.29	50.3	56.8	54.37
AttriCLIP + Ours	**61.7**	**55.89**	**62.91**	**60.2**
AttriCLIP + Ours (w/o init.)	61.33	54.95	62.14	59.86
AttriCLIP + Ours (w/o reg.)	58.95	52.6	60.04	57.93

Table 17: **Results for computationally budgeted CL setup [23]:** we follow the "Normal" budget setup from [23] where each incremental task is allocated training iterations equivalent of 1 epoch on the first task of each dataset. Scores reported are averages over three runs. Best results are in **bold**.

C Ablation studies

C.1 Sensitivity to the number of Monte Carlo (MC) samples.

We vary the number of MC samples M from 1 to 50. In Fig. 9, the accuracy is poorer in range $[1, 10]$, grows in range $[10, 20]$, and saturates thereafter. Hence, we set M to 20 for all our experiments.

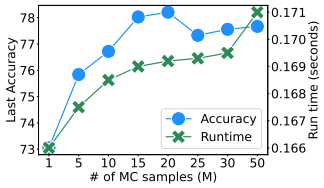

Figure 9: Accuracy-runtime trade-off with number of MC samples M.

C.2 Effect of forgetting on individual task adapters.

We ablate the task head predictions over the test set of each task on CIFAR100 (see App. C.2 for more details). Fig. 10a reports the accuracy of test set samples corresponding to the task encoder heads at the end of incremental training on the last task. Here, the first row is to be interpreted as follows: 77% of test samples belonging to test set of the first task (test set ID 1) were *correctly* allocated to task head 1, 1.4% of test samples belonging to test set of the first task (test set ID 1) were *incorrectly* allocated to task head 2, and so on. Visualizing the task head selection results for the last task evaluation helps us uncover the amount of forgetting among the individual task heads at the end of the incremental training.

Fig. 10b compares the evolution of the task head selection accuracy across the incremental test steps. Here, at the first test step, we have only one task head and thus the task head selection accuracy is 100%. At the second test step, we have the test samples from two seen tasks as well as two available

https://doi.org/10.52202/079017-4102

task heads. Out of all test samples of task 1, the reported 94.5% were correctly classified into the task head 1 while the rest 5.5% were incorrectly classified into the task head 2. Similarly, for test samples belonging to task 2, 3.1% were incorrectly classified into the task head 1 while the reported 96.9% were correctly classified into the task head 2, and so on. Hence, by studying the task head selection per incremental step, we can investigate the trend of forgetting among the individual task heads.

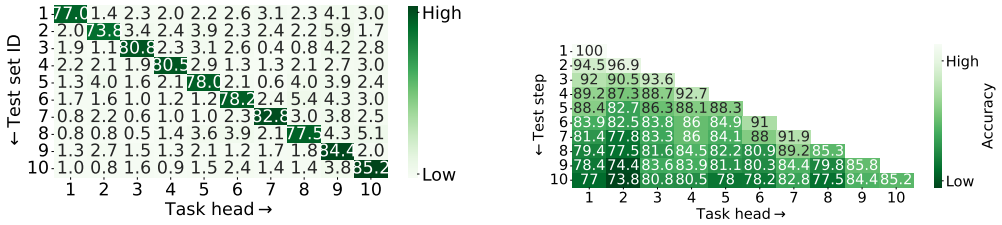

(a) Last step task head selection accuracies (b) Per step task head selection accuracies

Figure 10: **Task head selection accuracies** reported on CIFAR-100 upon: (a) evaluation on the last step, (b) evaluation on each incremental step.

C.3 Effect of inference module architecture.

To further investigate the effects of inference modules on performances, we vary the number of layers for the VGA module (sec. 3.2.2) and for the task-specific encoders (sec. 3.2.3). Fig. 11a reports the results of varying the number of Transformer Decoder layers [48] in the VGA module. As the number of layers grow, the average accuracy (Avg) increases while the last task accuracy (Last) decreases. This indicates that while a larger number of layers in the VGA module lead to an increase in the initial tasks' performances, these are amenable to larger forgetting on latter incremental steps.

In Fig. 11b, we report the performances for varying number of MLP layers in the mean and the standard deviation heads of the task distribution encoders. Unlike the VGA module, here we observe a consistent trend of decreasing last and average task accuracy with the increase in the number of layers. This clearly indicates the superiority of using a single-layered task distribution encoder.

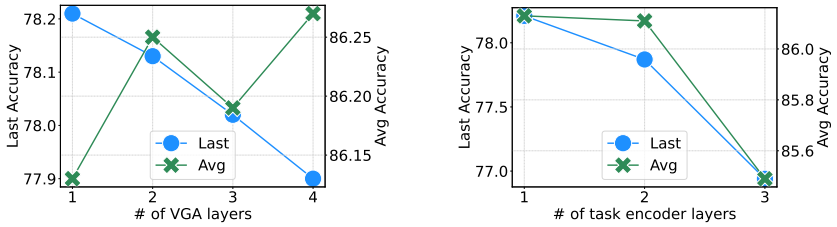

(a) (b)

Figure 11: **Ablation studies on CIFAR100 showing:** (a) the variation of accuracy with the number of Transformer decoder layers in the VGA module, (b) the variation of accuracy with the number of linear layers in the task-specific mean and standard deviation encoders.

C.4 Effect of prior type.

To study the role of a more informed prior in our VI framework, we study three choices of priors to be used in the prior-matching term of eq. (10): (a) the static (standard normal) prior, (b) the language-aware prior using the distribution obtained from the task encoders using the hand-crafted prompts' features $\{\mathbf{t}_y^{h,l}\}_{l=1}^{L}$ (sec 3.3), (c) the data-driven prior using a randomly chosen subset of a training minibatch as the context set to condition the prior on (see App. G for more details). App. Table 18 shows that while (b) and (c) slightly improve over (a) in terms of accuracies and forgetting, these come at the cost of poorer model calibration and longer runtime per iteration.

Prior type	Last ↑	Avg ↑	BwT ↑	ECE ↓	Runtime per iter. ↓
Static	78.21	86.13	-0.141	**0.204**	**0.169**
Data-driven	78.32	86.15	-0.115	0.216	0.172
Language-aware	**78.38**	**86.22**	**-0.112**	0.214	0.17

Table 18: **Performances of different priors** averaged over 3 runs on CIFAR100.

C.5 Inference time for different finetuning methods.

Table 19 investigates the inference time per iteration for different methods. Among the compared prompt-based methods, the inference time for AttriCLIP [19] is notably the highest. This is because it relies on selecting test instance-conditioned prompt tokens from a pool of prompt tokens. The instance-specific prompts are fed to the text encoder which further outputs an equivalent number of instance-specific text features to be used in the derivation of logits through eq. 1. These operations increase the inference time of AttriCLIP beyond our proposed variants of CLAP4CLIP with hand-crafted prompts (Ours), class-conditioned prompts (CoOp + Ours), and multi-modal prompts (MaPLe + Ours) where the latter three outperform AttriCLIP significantly across all our settings.

Method	Inference time (s)
Continual-CLIP [14]	0.017
CoOp [12]	0.018
MaPLe [20]	0.035
AttriCLIP [19]	0.257
CLIP-Adapter [13]	0.019
Ours	0.163
CoOp + Ours	0.182
MaPLe + Ours	0.064
AttriCLIP + Ours	0.299

Table 19: Average inference time for different finetuning methods on CIFAR100.

C.6 Influence of language-aware knowledge components on training dynamics.

Continuing our ablations from sec. 4.2, here we visualize the effects of using language-aware pre-trained knowledge, *i.e.*, weight initialization and task distribution regularization on the training dynamics of our model. For thorough analyses, we consider four variants of our model: (a) Ours uses both weight initialization and task distribution regularization, (b) Ours without weight initialization, (c) Ours without task distribution regularization, and (d) Ours without either of the language-aware components.

Does language-aware weight initialization help alleviate stability gap [57]? To answer this, we first investigate the evolution of the training loss during the initial training stages of each incremental task. Fig. 14 shows the loss $\mathcal{L}$ (Sec. 3.4) during the initial 100 training iterations of each task. We observe that our proposed weight initialization technique leads to lower training losses for the scenarios with or without task distribution regularization, *i.e.*, in general, **red values** $<$ **green values** and **blue values** $<$ **orange values**. Following [58], our observations support the hypothesis that larger loss values lead to the **stability gap** [57] for CL, and that an informed weight initialization method can help tackle it by reducing the initial training loss.

To further verify the benefit of our proposed weight initialization strategy for reducing the stability gap, we ablate the accuracy evolution of the first task test samples during the early training stages of each task. Figures 12b and 12a contrast these for CIFAR100. In general, our proposed weight initialization strategy helps mitigate the drop in accuracy during the initial training phases. On average, the first task accuracy upon the first iteration of training across all tasks remains 78.12 without weight initialization and grows to 79.5 with weight initialization, *i.e.,* a gain of 1.38 percentage points.

How does language-aware knowledge help learning of task distributions in general? To understand the effect of language-aware knowledge on task distribution learning, we next investigate the evolution of the means and standard deviations learned by the past and the new task heads throughout

https://doi.org/10.52202/079017-4102

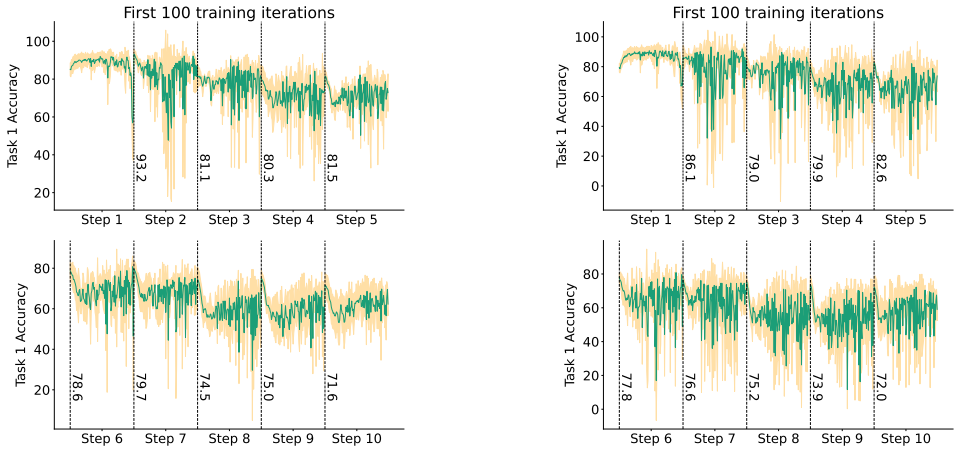

(a) With weight initialization

(b) Without weight initialization

Figure 12: **Effect of weight initialization on stability gap:** Test accuracy *with* and *without* weight initializations on the first task for the initial 100 iterations of incremental training on all ten tasks of CIFAR100. The green lines are the means over three different runs, the orange shades denote ± 1 standard error of the mean. The labels to the vertical bars denote the accuracy values for the first iteration of training on each task.

the training iterations. To this end, Fig. 15 and Fig. 16 report the training iterations against the L2 norm of means and standard deviations for the past task heads (at each incremental training step) and the new task heads (at each training step). We observe two consistent trends regarding the evolution of distributions of the past and the new task heads. First, the proposed initialization of weights helps stabilize the learning of the means and standard deviations with (**red** against **green**) or without (**blue** against **orange**) regularizing the task distributions. Second, regularizing the task distributions increases the L2 norms of the learned mean and the standard deviation as these now have to encode more information to mimic the distributions of the hand-crafted text features.

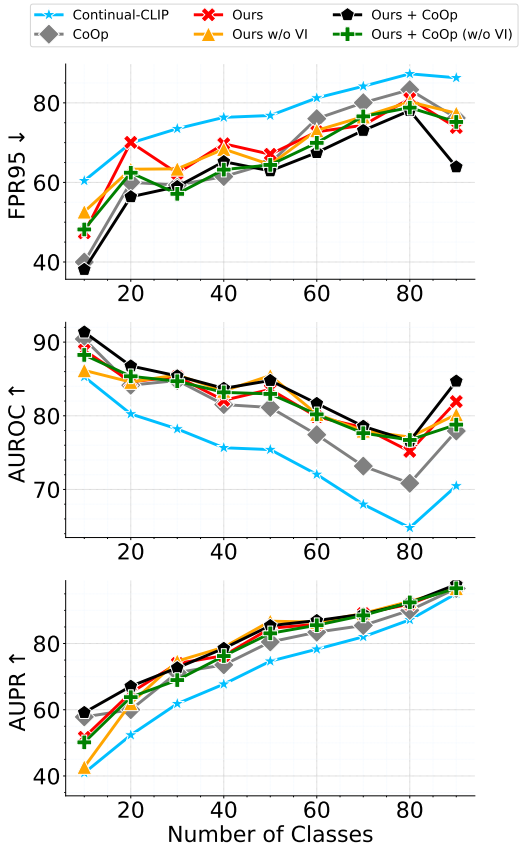

Figure 13: **Performance comparisons for post-hoc novel data detection** averaged over 3 runs on CIFAR100: FPR95 (**left**), AUROC (**middle**), and AUPR (**right**). The evaluations are carried over all but the last incremental test step.

D Out-of-the-box utilities of probabilistic finetuning

D.1 Post-hoc novel data detection

Our post-hoc novel data detection (PhNDD) setting aims to evaluate the continual learning methods at identifying novel data on the fly. To do so, we design an evaluation setup that uses no additional data resource other than that provided by the dataset-specific CL setting. Starting from the first test step, we treat the test data of the future tasks as *novel* while those of the seen tasks (including the most recently trained one) as *seen*. Since the last test step of a CL dataset has no future tasks, we exclude this step for our PhNDD evaluation, *i.e.,* we carry our PhNDD evaluation of CL models starting from the first until the penultimate test step.

Following other standard practices [75, 72], we use the Energy scores [75] of the outputs for each test sample as a measure of the model's confidence score. The samples assigned with a confidence score below the pre-defined confidence threshold are classified as novel. By assuming the seen data as the positive class and the novel data as the negative class, we can obtain a series of true positives rate (TPR) and false positive rate (FPR) by varying the confidence thresholds. One of our PhNDD evaluation metrics – the FPR95 then measures the FPR when the TPR is 0.95. As such, a lower FPR95 score indicates better PhNDD performance. Our other two PhNDD performance metrics include the the area under receiver operating characteristic curve (AUROC [73]) calculated based on FPR and TPR, and the precision-recall curve (AUPR [74]). Higher values of AUROC and AUPR indicate better PhNDD performance.

https://doi.org/10.52202/079017-4102

Table 4 reports the PhNDD metrics averaged over all the evaluated steps. Here, in Fig. 13, we show the evolution of these metrics with each evaluation starting from the first test step until the penultimate test step of CIFAR100. We observe that the zero-shot Continual-CLIP [14] has the poorest PhNDD performances (highest FPR95, and least AUROC and AUPR scores) across all steps given that it has not been finetuned on the downstream CL tasks. Among the finetuned methods, the CoOp [12] exhibits the poorest performances across all tasks. Among the variants of our method, combining CoOp with ours (CoOp + Ours) achieves the best PhNDD performances across all tasks. Furthermore, the deterministic versions: Ours w/o VI and CoOp + Ours (w/o VI) remain sub-optimal to their respective probabilistic variants, i.e., Ours and CoOp + Ours. The latter results validate the added perks of our probabilistic modeling framework for post-hoc novel data detection.

D.2 Exemplar selection results

Method	Avg	Last
CoOp	76.71	64.1
Clip-Adapter	78.78	68.49
Ours w/o VI	84.44	76.55
Ours	85.18	77.92

Table 20: **Entropy-based** exemplar selection results for different methods on CIFAR100.

E Limitations and further research directions

Few potential directions of research for CLAP4CLIP include the design of: (a) parameter-efficient adapters [85] for very large CL settings; (b) better regularization techniques to alleviate forgetting; and (c) more informed [86] yet computationally efficient priors for inference. Similarly, along the direction of alleviating forgetting and mitigating the stability gap [57, 58], it would be interesting to see how class-specific prompts generated by pre-trained Large Language Models (LLMs) can be exploited to obtain task-relevant language-aware CLIP knowledge while preserving the zero-shot transfer ability of the learned prompts (see App. Table 21 for a preliminary investigation). Lastly, we consider applying CLAP4CLIP to more sophisticated Vision-Language tasks [87] as another possible direction for research. We elaborate further on each of these directions below.

Parameter overhead. For each incoming task, CLAP4CLIP initializes a new head consisting of $d \times d$ parameters where d is the output dimension of the CLIP model's encoder. For a very large number of real-world CL tasks, the number of finetunable parameters for CLAP4CLIP may thus become comparable to or larger than that of the pre-trained CLIP model's ≈ 150 million parameters. For example, using a VIT-B/16 encoder with $d = 512$ brings an overhead of $\approx 525,000$ new parameters with each incoming task. After having seen ≈ 300 new tasks, the number of CLAP parameters to be finetuned thus amount to ≈ 158 million, which is larger than the frozen CLIP itself, and thus defeats the purpose of finetuning at the first place. One solid future direction to use CLAP4CLIP for very large real-world CL settings could thus be introducing more strict parameter-efficiency measures [88, 89] and/or learning probabilistic adapters with low-rank weights [85].

Design choices. Other future directions for improving CLAP4CLIP could include the use of better regularization techniques to further prevent forgetting (see Table 13 for the current forgetting in CLAP), and the search for more informed yet computationally efficient priors (see Table 18 for the computational overhead attached with more informed priors).

LLM-generated class descriptions as language-aware knowledge. In Sec. 3.3, we proposed using the text features from hand-crafted prompts as language-aware CLIP knowledge to help alleviate forgetting. However, hand-crafted prompts require manual labelling of data which is not always practical. Hence, several recent works [90, 91, 92] have opted to mining Large Language Models (LLMs) for efficiently obtaining the class-specific descriptions. To study the feasibility of alleviating forgetting using such LLM-generated class descriptions, we leverage the diverse prompts from CuPL [91] obtained using the GPT-3 [93] model. Our preliminary investigation suggests that the

hand-crafted prompts have an upper hand over GPT-3 based prompts for CLAP4CLIP performance (see Table 21). This could be because of the broad range of knowledge encoded in the GPT-generated prompts – which at times are irrelevant for the test images.

Prompt type	Last ↑	Avg ↑	BwT ↑	ECE ↓	Runtime per iter. ↓
Hand-crafted	**78.21**	**86.13**	-0.141	**0.204**	0.169
GPT-3	77.76	85.7	**-0.099**	0.219	**0.151**

Table 21: **Performance comparison on CIFAR100** using hand-crafted vs. LLM-generated prompts for encoding language-aware CLIP knowledge. The results reported are averages over 3 runs. Best results across the metrics are highlighted in **bold**.

Based on the above finding, we suggest leveraging task-relevant LLM-generated descriptions as language-aware knowledge to be another promising future research direction. It is worth noting that a number of existing methods that rely on LLM-generated prompts are limited in their transferable knowledge across unseen classes and datasets [90, 91] (e.g., any new class at test-time would require mining the LLM descriptions in advance). On the contrary, our proposed weight initialization and task distribution regularization strategies provide a natural framework for LLM-generated prompts to be used alongside arbitrary learnable prompts (e.g. replacing $\mathbf{t}_y^{h,l}$ in eq. (7)). This compliments the idea of LLM-based text-only supervision frameworks [92] that seek to enrich *zero-shot transfer* of prompts to new classes by extracting rich contextual information from LLM data.[3]

Compatibility with Vision-Language datasets The tasks we have covered so far in the paper are based solely on Vision datasets. To further demonstrate that our method is compatible with more sophisticated vision-language datasets, we here consider using a toy Visual Question Answering (VQAv2) task from the CLiMB dataset [87]. The CLiMB dataset hosts a number of tasks/settings to evaluate multi-modal and low-shot transfer abilities of CL algorithms. However, given the intricacies of these tasks (visual question answering, reasoning, etc.), we leave a full in-depth engagement with CLiMB [87] as a separate future direction for research.[4]

To show the aptness of our method for the dataset's tasks, we carry out preliminary experiments on the single-task learning setting [94] of the VQAv2 subset of CLiMB. Following [94], we rely on the BART model [95] for text generation here. Table 22 shows that our method surpasses the Continual-CLIP by 9.29 percentage points on the VQAv2 task, thus showing that ours enhances the zero-shot generalization capability of CLIP.

Model	VQAv2 task score
Continual-CLIP	57.42
Ours	66.71

Table 22: Single-task learning performance on the VQAv2 subset of the CLiMB dataset.

E.1 Broader Impact

Recent years have witnessed the immense popularity of sequential generative models like Stable Diffusion [10] with applications in multimodal content generation as well as scientific research through fast and highly detailed sampling. The CLIP text encoder is widely employed by such generative models for learning personalized concepts conditioned on text prompts [96, 97]. By effective continual finetuning of the text encoder's features, our method can thus aid in customizing such models in a sequential manner using multiple, fine-grained concepts [98, 26].

[3]Given that new classes might emerge at test time for which we do not have the LLM-generated descriptions, it is important that the learned prompts preserve their zero-shot generalization ability.

[4]The CLiMB dataset [87] was introduced as an independent CL benchmark with a number of tasks (Visual Question Answering/Reasoning/Entailment) and training settings including low-shot and unimodal learning. Existing works [94] that study CLiMB thus rely solely on it *and not on additional datasets* for evaluations.

https://doi.org/10.52202/079017-4102

F Derivation of ELBO for the static prior.

We seek to maximize the likelihood $p(y^{1:T})$ for all observed labels $y^{1:T}$. To derive the predictions, our framework uses the visual-aligned text features $\tilde{\mathbf{t}}_c^{1:T}$ and the image inputs $\mathbf{x}$ (see eq. (1)). Our evidence is thus $p(y^{1:T}|\mathbf{x};\tilde{\mathbf{t}}_c^{1:T})$ for which we derive the lower bound (ELBO). In the following, we denote the prior network as $p_\theta(z^t)$ for which the true posterior is $p_\theta(z^t|\mathbf{x};\tilde{\mathbf{t}}_c^t)$. We approximate the true posterior using the variational posterior $q_\phi(z^t|\mathbf{x};\tilde{\mathbf{t}}_c^t)$. Our derivation ends up with the reconstruction term $p_\theta(y^t|z^t,\mathbf{x};\tilde{\mathbf{t}}_c^t)$ that can be seen as a deterministic function converting a given latent vector z^t and an input image $\mathbf{x}$ into an observation y^t. For our CLIP-based variational framework, this deterministic function is the cosine similarity operation followed by the softmax application (Eq. (3b)).

$$
\begin{aligned}
&\log\, p_\theta(y^{1:T}|\mathbf{x};\tilde{\mathbf{t}}_c^{1:T}) && \text{(Log-likelihood of evidence)}\\
&= \log p_\theta(y^{1:T}|\mathbf{x};\tilde{\mathbf{t}}_c^{1:T}) \int q_\phi(z^{1:T}|\mathbf{x};\tilde{\mathbf{t}}_c^{1:T})dz^{1:T} && (\because \int q_\phi(z^{1:T}|x^{1:T})dz^{1:T}=1)\\
&= \int q_\phi(z^{1:T}|\mathbf{x};\tilde{\mathbf{t}}_c^{1:T})\big(\log p_\theta(y^{1:T}|\mathbf{x};\tilde{\mathbf{t}}_c^{1:T})\big)dz^{1:T} && \text{(Bring evidence into integral)}\\
&= \mathbb{E}_{q_\phi(z^{1:T}|\mathbf{x};\tilde{\mathbf{t}}_c^{1:T})}\big[\log p_\theta(y^{1:T}|\mathbf{x};\tilde{\mathbf{t}}_c^{1:T})\big] && \text{(Definition of Expectation)}\\
&= \sum_{t=1}^{T}\Big[\mathbb{E}_{q_\phi(z^t|\mathbf{x};\tilde{\mathbf{t}}_c^t)}\big[\log p_\theta(y^t|\mathbf{x};\tilde{\mathbf{t}}_c^t)\big]\Big] && \text{(Rewrite using sum)}\\
&= \sum_{t=1}^{T}\Big[\mathbb{E}_{q_\phi(z^t|\mathbf{x};\tilde{\mathbf{t}}_c^t)}\big[\log \frac{p_\theta(y^t,z^t|\mathbf{x};\tilde{\mathbf{t}}_c^t)}{p_\theta(z^t|\mathbf{x};\tilde{\mathbf{t}}_c^t)}\big]\Big] && \text{(Re-introduce } z^t \text{ by Chain rule of probability)}\\
&= \sum_{t=1}^{T}\Big[\mathbb{E}_{q_\phi(z^t|\mathbf{x};\tilde{\mathbf{t}}_c^t)}\big[\log \frac{p_\theta(y^t,z^t|\mathbf{x};\tilde{\mathbf{t}}_c^t)q_\phi(z^t|\mathbf{x};\tilde{\mathbf{t}}_c^t)}{p_\theta(z^t|\mathbf{x};\tilde{\mathbf{t}}_c^t)q_\phi(z^t|\mathbf{x};\tilde{\mathbf{t}}_c^t)}\big]\Big] && (\text{Multiply by } 1=\frac{q_\phi(z^t|\mathbf{x};\tilde{\mathbf{t}}_c^t)}{q_\phi(z^t|\mathbf{x};\tilde{\mathbf{t}}_c^t)})\\
&= \sum_{t=1}^{T}\Big[\mathbb{E}_{q_\phi(z^t|\mathbf{x};\tilde{\mathbf{t}}_c^t)}\big[\log \frac{p_\theta(y^t,z^t|\mathbf{x};\tilde{\mathbf{t}}_c^t)}{q_\phi(z^t|\mathbf{x};\tilde{\mathbf{t}}_c^t)}\big] + \mathbb{E}_{q_\phi(z^t|\mathbf{x};\tilde{\mathbf{t}}_c^t)}\big[\log \frac{q_\phi(z^t|\mathbf{x};\tilde{\mathbf{t}}_c^t)}{p_\theta(z^t|\mathbf{x};\tilde{\mathbf{t}}_c^t)}\big]\Big] && \text{(Split the expectation)}\\
&= \sum_{t=1}^{T}\Big[\mathbb{E}_{q_\phi(z^t|\mathbf{x};\tilde{\mathbf{t}}_c^t)}\big[\log \frac{p_\theta(y^t,z^t|\mathbf{x};\tilde{\mathbf{t}}_c^t)}{q_\phi(z^t|\mathbf{x};\tilde{\mathbf{t}}_c^t)}\big] + \mathbb{D}_{\text{KL}}\big(q_\phi(z^t|\mathbf{x};\tilde{\mathbf{t}}_c^t)\|p_\theta(z^t|\mathbf{x};\tilde{\mathbf{t}}_c^t)\big)\Big] && \text{(Definition of KL divergence)}\\
&\geq \sum_{t=1}^{T}\Big[\mathbb{E}_{q_\phi(z^t|\mathbf{x};\tilde{\mathbf{t}}_c^t)}\big[\log \frac{p_\theta(y^t,z^t|\mathbf{x};\tilde{\mathbf{t}}_c^t)}{q_\phi(z^t|\mathbf{x};\tilde{\mathbf{t}}_c^t)}\big]\Big] && (\because \text{ KL divergence} \geq 0)\\
&\geq \sum_{t=1}^{T}\Big[\mathbb{E}_{q_\phi(z^t|\mathbf{x};\tilde{\mathbf{t}}_c^t)}\big[\log \frac{p_\theta(y^t|z^t,\mathbf{x};\tilde{\mathbf{t}}_c^t)p_\chi(z^t)}{q_\phi(z^t|\mathbf{x};\tilde{\mathbf{t}}_c^t)}\big]\Big] && \text{(Chain rule of probability)}\\
&\geq \sum_{t=1}^{T}\Big[\mathbb{E}_{q_\phi(z^t|\mathbf{x};\tilde{\mathbf{t}}_c^t)}\big[\log p_\theta(y^t|z^t,\mathbf{x};\tilde{\mathbf{t}}_c^t)\big] + \mathbb{E}_{q_\phi(z^t|\mathbf{x};\tilde{\mathbf{t}}_c^t)}\big[\frac{p_\chi(z^t)}{q_\phi(z^t|\mathbf{x};\tilde{\mathbf{t}}_c^t)}\big]\Big] && \text{(Split the Expectation)}\\
&\geq \sum_{t=1}^{T}\Big[\mathbb{E}_{q_\phi(z^t|\mathbf{x};\tilde{\mathbf{t}}_c^t)}\big[\log p_\theta(y^t|z^t,\mathbf{x};\tilde{\mathbf{t}}_c^t)\big] - \mathbb{D}_{\text{KL}}\big(q_\phi(z^t|\mathbf{x};\tilde{\mathbf{t}}_c^t)\|p_\chi(z^t)\big)\Big] && \text{(Definition of KL divergence)}
\end{aligned}
$$

G Data-driven prior

The choice of prior is pivotal to a Bayesian inference workflow like ours [99]. While a standard Gaussian prior $p_\chi = \mathcal{N}(0, I)$ adapts well to a range of settings, it is (seemingly) uninformative regarding the nature of a given task [100]. With the end goal of deriving more informative priors, we thus seek to replace p_χ with task data-dependent prior distributions p^t, wherever applicable.

To this end, we first note that the outputs of the VGA module remain **invariant** not only to the order of the input text features (due to self-attention) but also to the order of the contextual image features (due to cross-attention). The latter invariance implies that the joint task-specific distribution learned by the encoder q_ϕ^t (conditioned on the VGA outputs $\hat{\mathbf{t}}_c^t$ from eq. 5a) is preserved if we were to permute the elements of the task-specific visual context set. More formally, this observation helps guarantee the (finite) *exchangeability* and the *consistency* properties of a stochastic process [101].

Motivated by the above, we treat the $t-$th task image features $\mathbf{x}^t$ as the target set $\mathcal{T}^t$ and employ a randomly chosen subset of it as our context set $\mathcal{C}^t$ to align the $t-$th task text features and to condition our prior p^t on:

$$
\begin{aligned}
\hat{\mathbf{t}}_c^t &= \text{VGA}\big(Q=\mathbf{t}_c^t, K=V=\mathcal{C}^t\big),\\
p^t &= q_\phi^t(\tilde{\mathbf{t}}_c^t) = \big(\mu^t(\tilde{\mathbf{t}}_c^t), \sigma^t(\tilde{\mathbf{t}}_c^t)\big)
\end{aligned}
\tag{12}
$$

where $\tilde{\mathbf{t}}^t$ is the fused task-specific text feature following eq. (5b). The task-specific prior p^t thus endows our training framework with a resemblance to the neural process (NP) architectures

[102, 103, 8]. Following NPs, we use the same encoder q_ϕ^t to parameterize the conditional prior and the variational posterior. This results in the following approximate ELBO (see App. F for the ELBO derivation):

$$\begin{aligned}\log p(\mathbf{y}^{1:T}|\mathbf{x}, \mathcal{C}^{1:T}) \geq \\ \sum_{t=1}^{T} \Bigg[\mathbb{E}_{q_\phi(z^t|\mathbf{x})} \Big[\log p(\mathbf{y}^t|z^t, \mathbf{x}_{\mathcal{T}}^t, \mathcal{C}^t) \Big] \\ - \mathbb{D}_{\mathrm{KL}} \big(q_\phi(z^t|\mathcal{T}^t) \| q_\phi(z^t|\mathcal{C}^t) \big) \Bigg]\end{aligned} \tag{13}$$

where in practice, the entire set of $t-$th images in a training minibatch form the target set $\mathcal{T}^t$ and a randomly chosen subset of the targets make up the context $\mathcal{C}^t$ [104]. Note that *unlike* NPs, our framework does not entirely rely on data-driven priors. Namely, while training on a CL task t, the past-task encoders are frozen and we have ample $t-$th task data points to condition the prior on. We thus resort to optimizing the ELBO (13) during training. On the other hand, during finetuning, we have limited task-specific data points to condition our context on. As such, we empirically found that switching to the static prior yields better results and thus resort to optimizing the ELBO (10) during finetuning.

G.1 Effect of the context size on data-driven prior.

Table 18 in the main paper compares the results of using a data-driven prior against the uniform normal prior and the language-aware prior (see Sec. 3.3), where the latter is driven from the pre-trained text encoder using hand-crafted prompts. We observe that data-driven prior leads to minor accuracy improvements over the standard normal prior but falls narrowly behind the language-aware prior. Here, we study the influence of the batch size of the context set selected at random to derive our prior from.

Table 23 shows the last task accuracy with varying context sizes and a fixed target batch size of 64. We find that a smaller context set size hurts the performance of the model to the extent of falling behind the standard normal prior. Given that the context sets are the sampled subsets of the training (target) minibatches, a much smaller context set can lead to the increase in the prior matching loss values. We find that the context set batch size of 40 performs the best, and thus use this to ablate the prior-dependent performances in the main paper.

	4	8	16	32	40	50	Static prior
Accuracy	76.1	76.99	77.41	78.03	78.32	77.35	78.21

Table 23: **Influence of the context set size** used to derive the data-driven prior on CIFAR100.

G.2 Derivation of ELBO for the data-driven prior.

Similar to App. F, we start with the log-likelihood of the evidence which now involves conditioning on an additional context set $\mathcal{C}^{1:T}$. The $t-$th task context set is used to condition our prior network $p_\theta(z^t|\mathcal{C}^t)$. Following the standard practices of other data-driven prior frameworks [102, 8], we introduce parameter-sharing between our conditional prior and variational posterior networks. This allows us to replace our prior network with the variational posterior network $q_\phi(z^t|\mathcal{T}^t)$, where $\mathcal{T}$ is

https://doi.org/10.52202/079017-4102

the target set for task t.

$$
\begin{aligned}
&\log\, p_\theta(Y_{\mathcal{T}}^{1:T}|\mathbf{x}_{\mathcal{T}}^{1:T}, \mathcal{C}^{1:T}) && \text{(Log-likelihood of evidence)}\\
&= \log p_\theta(Y_{\mathcal{T}}^{1:T}|\mathbf{x}_{\mathcal{T}}^{1:T}, \mathcal{C}^{1:T}) \int q_\phi(z^{1:T}|\mathbf{x}_{\mathcal{T}}^{1:T}, \mathcal{C}^{1:T}) dz^{1:T} && \left(\because \int q_\phi(z^{1:T}|\mathbf{x}_{\mathcal{T}}^{1:T}, \mathcal{C}^{1:T}) dz^{1:T} = 1\right)\\
&= \int q_\phi(z^{1:T}|\mathbf{x}_{\mathcal{T}}^{1:T}, \mathcal{C}^{1:T}) \big(\log p_\theta(Y_{\mathcal{T}}^{1:T}|\mathbf{x}_{\mathcal{T}}^{1:T}, \mathcal{C}^{1:T})\big) dz^{1:T} && \text{(Bring evidence into integral)}\\
&= \mathbb{E}_{q_\phi(z^{1:T}|\mathcal{T}^{1:T})}[\log p_\theta(Y_{\mathcal{T}}^{1:T}|\mathbf{x}_{\mathcal{T}}^{1:T}, \mathcal{C}^{1:T})] && \text{(By definition)}\\
&= \sum_{t=1}^{T} \Big[\mathbb{E}_{q_\phi(z^t|\mathcal{T}^t)}[\log p_\theta(Y_{\mathcal{T}}^{t}|\mathbf{x}_{\mathcal{T}}^{t}, \mathcal{C}^{t})]\Big] && \text{(Rewrite using sum)}\\
&= \sum_{t=1}^{T} \Big[\mathbb{E}_{q_\phi(z^t|\mathcal{T}^t)}\Big[\log \frac{p_\theta(Y_{\mathcal{T}}^{t}, z^t|\mathbf{x}_{\mathcal{T}}^{t}, \mathcal{C}^{t})}{p_\theta(z^t|\mathbf{x}_{\mathcal{T}}^{t}, Y_{\mathcal{T}}^{t}, \mathcal{C}^{t})}\Big]\Big] && \text{(Re-introduce } z^t \text{ by Chain rule of probability)}\\
&= \sum_{t=1}^{T} \Big[\mathbb{E}_{q_\phi(z^t|\mathcal{T}^t)}\Big[\log \frac{p_\theta(Y_{\mathcal{T}}^{t}|z^t, \mathbf{x}_{\mathcal{T}}^{t}, \mathcal{C}^{t})\; p_\theta(z^t|\mathcal{C}^t)}{p_\theta(z^t|\mathcal{T}^t)}\Big]\Big] && \text{(By Chain rule of probability; } \mathcal{C} \subset \mathcal{T})\\
&= \sum_{t=1}^{T} \Big[\mathbb{E}_{q_\phi(z^t|\mathcal{T}^t)}\Big[\log \frac{p_\theta(Y_{\mathcal{T}}^{t}|z^t, \mathbf{x}_{\mathcal{T}}^{t}, \mathcal{C}^{t})\; p_\theta(z^t|\mathcal{C}^t)\; q_\phi(z^t|\mathcal{T}^t)}{p_\theta(z^t|\mathcal{T}^t)\; q_\phi(z^t|\mathcal{T}^t)}\Big]\Big] && \text{(Equivalent fraction)}\\
&= \sum_{t=1}^{T} \Big[\mathbb{E}_{q_\phi(z^t|\mathcal{T}^t)}\Big[\log p_\theta(Y_{\mathcal{T}}^{t}|z^t, \mathbf{x}_{\mathcal{T}}^{t}, \mathcal{C}^{t})\Big]\\
&\qquad + \mathbb{E}_{q_\phi(z^t|\mathcal{T}^t)}\Big[\log \frac{p_\theta(z^t|\mathcal{C}^t)}{q_\phi(z^t|\mathcal{T}^t)}\Big] + \mathbb{E}_{q_\phi(z^t|\mathcal{T}^t)}\Big[\log \frac{q_\phi(z^t|\mathcal{T}^t)}{p_\theta(z^t|\mathcal{T}^t)}\Big]\Big] && \text{(Split the expectation)}\\
&= \sum_{t=1}^{T} \Big[\mathbb{E}_{q_\phi(z^t|\mathcal{T}^t)}\Big[\log p_\theta(Y_{\mathcal{T}}^{t}|z^t, \mathbf{x}_{\mathcal{T}}^{t}, \mathcal{C}^{t})\Big]\\
&\qquad - \mathbb{D}_{\mathrm{KL}}\big(q_\phi(z^t|\mathcal{T}^t)\|p_\theta(z^t|\mathcal{C}^t)\big) + \mathbb{D}_{\mathrm{KL}}\big(q_\phi(z^t|\mathcal{T}^t)\|p_\theta(z^t|\mathcal{T}^t)\big)\Big] && \text{(By definition of KL divergence)}\\
&\geq \sum_{t=1}^{T} \Big[\mathbb{E}_{q_\phi(z^t|\mathcal{T}^t)}\Big[\log p_\theta(Y_{\mathcal{T}}^{t}|z^t, \mathbf{x}_{\mathcal{T}}^{t}, \mathcal{C}^{t})\Big] - \mathbb{D}_{\mathrm{KL}}\big(q_\phi(z^t|\mathcal{T}^t)\|p_\theta(z^t|\mathcal{C}^t)\big)\Big] && (\because \text{KL divergence} \geq 0)
\end{aligned}
$$

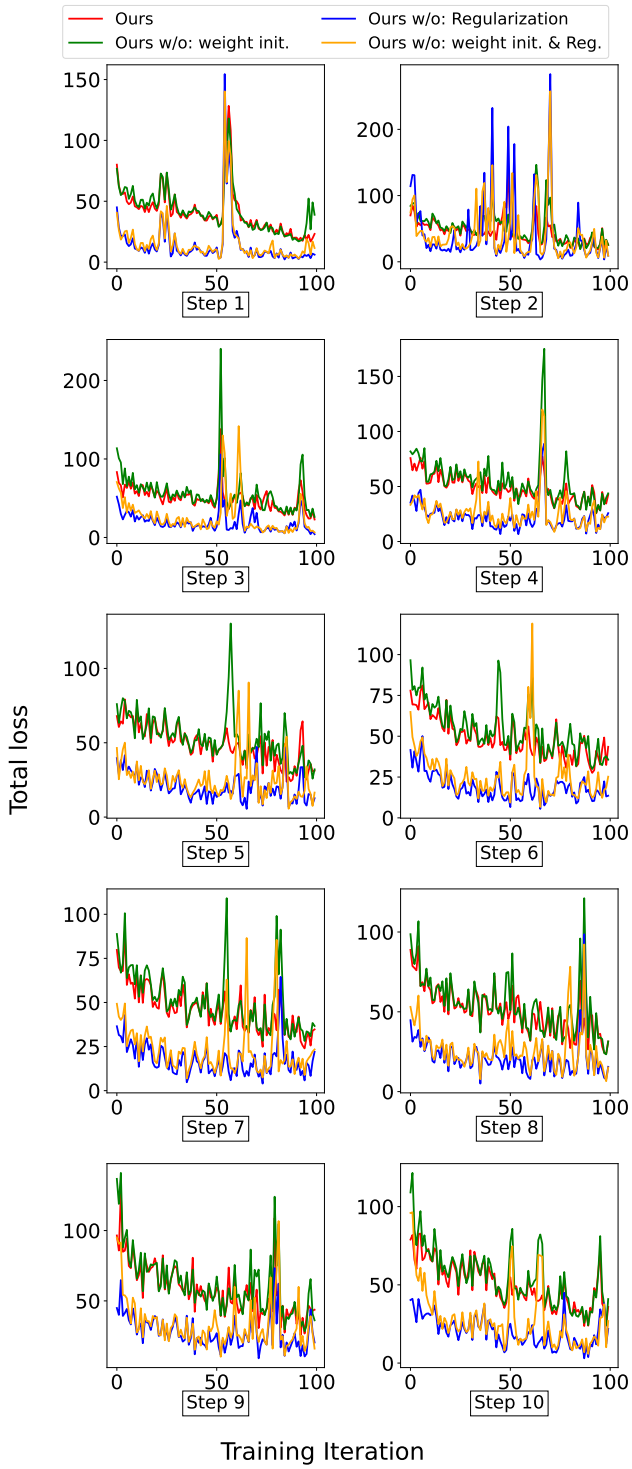

Figure 14: **Evolution of the loss value** $\mathcal{L}$ during the first 100 training iterations of each task on CIFAR100. Training with our proposed weight initialization strategy consistently leads to lower training losses thus bridging the **stability gap** [57] in CL.

https://doi.org/10.52202/079017-4102

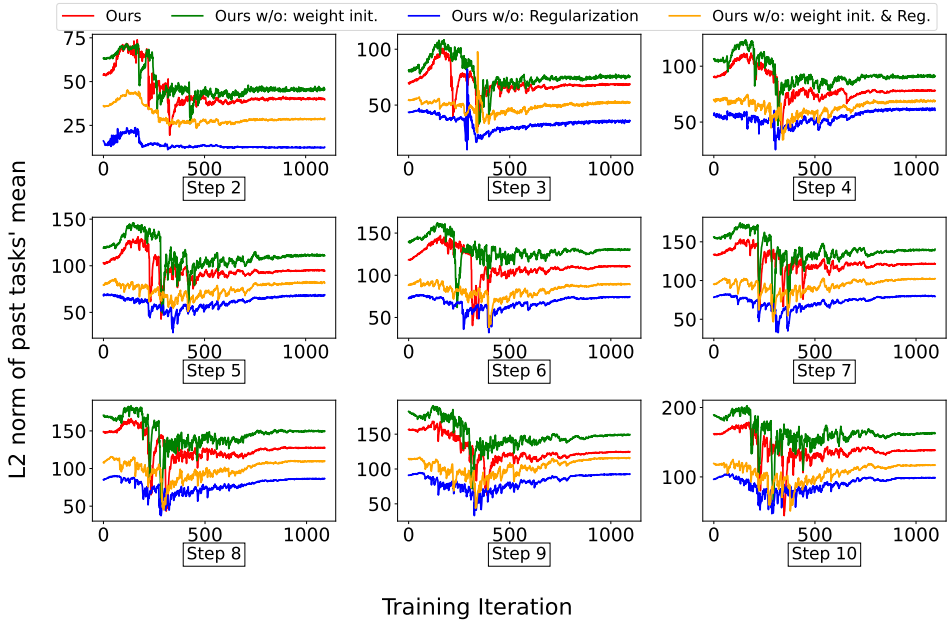

(a) L2 norm of mean of past task heads

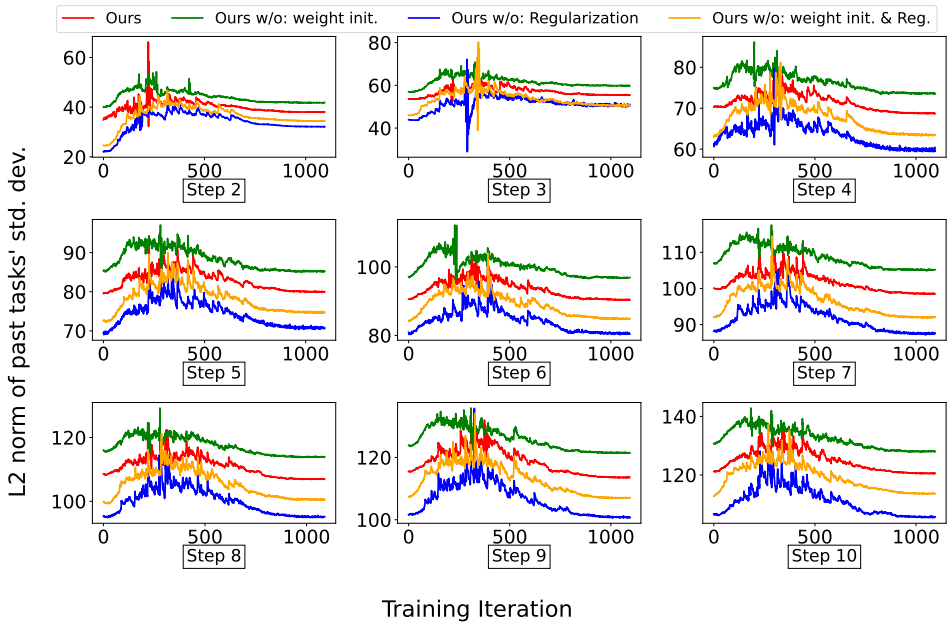

(b) L2 norm of standard deviation of past task heads

Figure 15: **Evolution of mean and standard deviation** of past task encoders with training iterations.

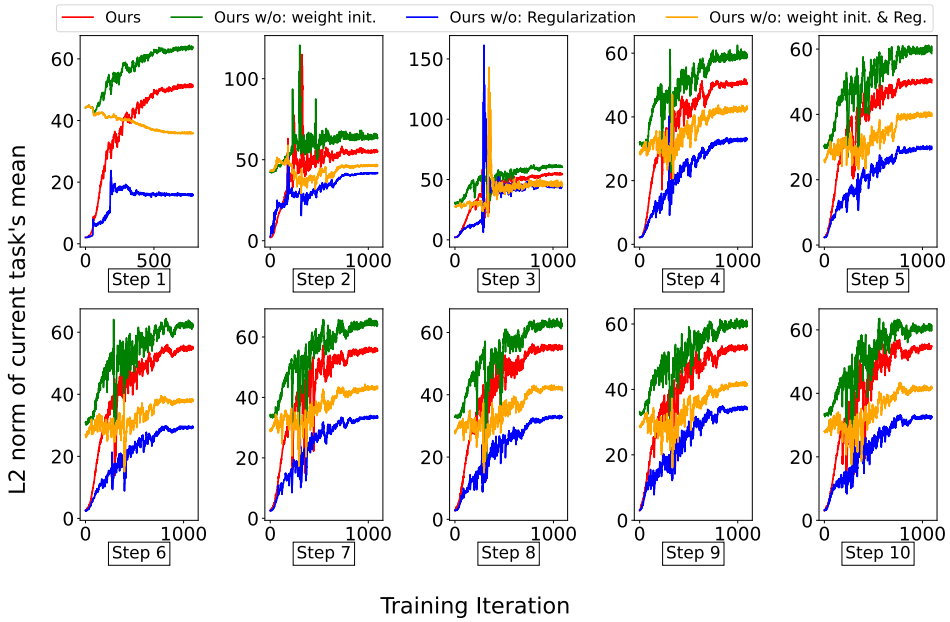

(a) L2 norm of mean of current task heads

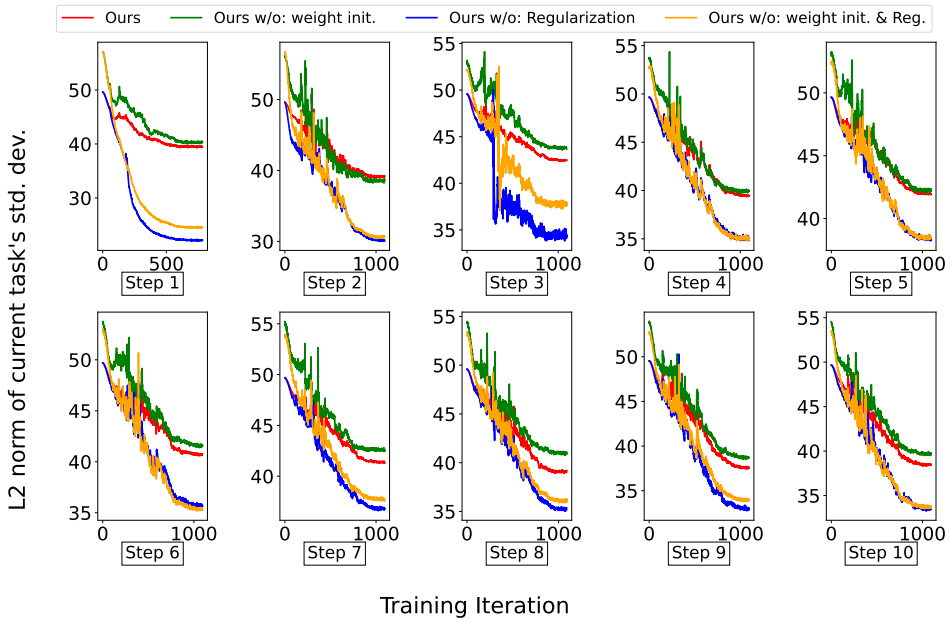

(b) L2 norm of standard deviation of current task heads

Figure 16: **Evolution of mean and standard deviation** of task encoders (recorded at the step where they were first introduced) with training iterations.

https://doi.org/10.52202/079017-4102

NeurIPS Paper Checklist

1. **Claims**

   Question: Do the main claims made in the abstract and introduction accurately reflect the paper's contributions and scope?

   Answer: [Yes]

   Justification: To support the claims, we provide in-depth experimental results on four different (with replay memory, cross-datasets, and resource-constrained) CL setups.

   Guidelines:

   - The answer NA means that the abstract and introduction do not include the claims made in the paper.
   - The abstract and/or introduction should clearly state the claims made, including the contributions made in the paper and important assumptions and limitations. A No or NA answer to this question will not be perceived well by the reviewers.
   - The claims made should match theoretical and experimental results, and reflect how much the results can be expected to generalize to other settings.
   - It is fine to include aspirational goals as motivation as long as it is clear that these goals are not attained by the paper.

2. **Limitations**

   Question: Does the paper discuss the limitations of the work performed by the authors?

   Answer: [Yes]

   Justification: We detail the limitations of our work in App. E. This includes parameter overhead and design choices.

   Guidelines:

   - The answer NA means that the paper has no limitation while the answer No means that the paper has limitations, but those are not discussed in the paper.
   - The authors are encouraged to create a separate "Limitations" section in their paper.
   - The paper should point out any strong assumptions and how robust the results are to violations of these assumptions (e.g., independence assumptions, noiseless settings, model well-specification, asymptotic approximations only holding locally). The authors should reflect on how these assumptions might be violated in practice and what the implications would be.
   - The authors should reflect on the scope of the claims made, e.g., if the approach was only tested on a few datasets or with a few runs. In general, empirical results often depend on implicit assumptions, which should be articulated.
   - The authors should reflect on the factors that influence the performance of the approach. For example, a facial recognition algorithm may perform poorly when image resolution is low or images are taken in low lighting. Or a speech-to-text system might not be used reliably to provide closed captions for online lectures because it fails to handle technical jargon.
   - The authors should discuss the computational efficiency of the proposed algorithms and how they scale with dataset size.
   - If applicable, the authors should discuss possible limitations of their approach to address problems of privacy and fairness.
   - While the authors might fear that complete honesty about limitations might be used by reviewers as grounds for rejection, a worse outcome might be that reviewers discover limitations that aren't acknowledged in the paper. The authors should use their best judgment and recognize that individual actions in favor of transparency play an important role in developing norms that preserve the integrity of the community. Reviewers will be specifically instructed to not penalize honesty concerning limitations.

3. **Theory Assumptions and Proofs**

   Question: For each theoretical result, does the paper provide the full set of assumptions and a complete (and correct) proof?

Answer: [Yes]

Justification: We detail the derivation of Evidence Lower Bound for our proposed model in App. F.

Guidelines:

- The answer NA means that the paper does not include theoretical results.
- All the theorems, formulas, and proofs in the paper should be numbered and cross-referenced.
- All assumptions should be clearly stated or referenced in the statement of any theorems.
- The proofs can either appear in the main paper or the supplemental material, but if they appear in the supplemental material, the authors are encouraged to provide a short proof sketch to provide intuition.
- Inversely, any informal proof provided in the core of the paper should be complemented by formal proofs provided in appendix or supplemental material.
- Theorems and Lemmas that the proof relies upon should be properly referenced.

4. **Experimental Result Reproducibility**

   Question: Does the paper fully disclose all the information needed to reproduce the main experimental results of the paper to the extent that it affects the main claims and/or conclusions of the paper (regardless of whether the code and data are provided or not)?

   Answer: [Yes]

   Justification: We have made our code public in addition to providing details on hyperparameter choices and tuning.

   Guidelines:

   - The answer NA means that the paper does not include experiments.
   - If the paper includes experiments, a No answer to this question will not be perceived well by the reviewers: Making the paper reproducible is important, regardless of whether the code and data are provided or not.
   - If the contribution is a dataset and/or model, the authors should describe the steps taken to make their results reproducible or verifiable.
   - Depending on the contribution, reproducibility can be accomplished in various ways. For example, if the contribution is a novel architecture, describing the architecture fully might suffice, or if the contribution is a specific model and empirical evaluation, it may be necessary to either make it possible for others to replicate the model with the same dataset, or provide access to the model. In general. releasing code and data is often one good way to accomplish this, but reproducibility can also be provided via detailed instructions for how to replicate the results, access to a hosted model (e.g., in the case of a large language model), releasing of a model checkpoint, or other means that are appropriate to the research performed.
   - While NeurIPS does not require releasing code, the conference does require all submissions to provide some reasonable avenue for reproducibility, which may depend on the nature of the contribution. For example
     (a) If the contribution is primarily a new algorithm, the paper should make it clear how to reproduce that algorithm.
     (b) If the contribution is primarily a new model architecture, the paper should describe the architecture clearly and fully.
     (c) If the contribution is a new model (e.g., a large language model), then there should either be a way to access this model for reproducing the results or a way to reproduce the model (e.g., with an open-source dataset or instructions for how to construct the dataset).
     (d) We recognize that reproducibility may be tricky in some cases, in which case authors are welcome to describe the particular way they provide for reproducibility. In the case of closed-source models, it may be that access to the model is limited in some way (e.g., to registered users), but it should be possible for other researchers to have some path to reproducing or verifying the results.

5. **Open access to data and code**

https://doi.org/10.52202/079017-4102

Question: Does the paper provide open access to the data and code, with sufficient instructions to faithfully reproduce the main experimental results, as described in supplemental material?

Answer: [Yes]

Justification: We use publicly available datasets and have also released our code.

Guidelines:

- The answer NA means that paper does not include experiments requiring code.
- Please see the NeurIPS code and data submission guidelines (`https://nips.cc/public/guides/CodeSubmissionPolicy`) for more details.
- While we encourage the release of code and data, we understand that this might not be possible, so "No" is an acceptable answer. Papers cannot be rejected simply for not including code, unless this is central to the contribution (e.g., for a new open-source benchmark).
- The instructions should contain the exact command and environment needed to run to reproduce the results. See the NeurIPS code and data submission guidelines (`https://nips.cc/public/guides/CodeSubmissionPolicy`) for more details.
- The authors should provide instructions on data access and preparation, including how to access the raw data, preprocessed data, intermediate data, and generated data, etc.
- The authors should provide scripts to reproduce all experimental results for the new proposed method and baselines. If only a subset of experiments are reproducible, they should state which ones are omitted from the script and why.
- At submission time, to preserve anonymity, the authors should release anonymized versions (if applicable).
- Providing as much information as possible in supplemental material (appended to the paper) is recommended, but including URLs to data and code is permitted.

6. **Experimental Setting/Details**

   Question: Does the paper specify all the training and test details (e.g., data splits, hyperparameters, how they were chosen, type of optimizer, etc.) necessary to understand the results?

   Answer: [Yes]

   Justification: We detail these in App. A.2.

   Guidelines:

   - The answer NA means that the paper does not include experiments.
   - The experimental setting should be presented in the core of the paper to a level of detail that is necessary to appreciate the results and make sense of them.
   - The full details can be provided either with the code, in appendix, or as supplemental material.

7. **Experiment Statistical Significance**

   Question: Does the paper report error bars suitably and correctly defined or other appropriate information about the statistical significance of the experiments?

   Answer: [Yes]

   Justification: We report the standard deviation scores for our main results in Table 12.

   Guidelines:

   - The answer NA means that the paper does not include experiments.
   - The authors should answer "Yes" if the results are accompanied by error bars, confidence intervals, or statistical significance tests, at least for the experiments that support the main claims of the paper.
   - The factors of variability that the error bars are capturing should be clearly stated (for example, train/test split, initialization, random drawing of some parameter, or overall run with given experimental conditions).
   - The method for calculating the error bars should be explained (closed form formula, call to a library function, bootstrap, etc.)

- The assumptions made should be given (e.g., Normally distributed errors).
- It should be clear whether the error bar is the standard deviation or the standard error of the mean.
- It is OK to report 1-sigma error bars, but one should state it. The authors should preferably report a 2-sigma error bar than state that they have a 96% CI, if the hypothesis of Normality of errors is not verified.
- For asymmetric distributions, the authors should be careful not to show in tables or figures symmetric error bars that would yield results that are out of range (e.g. negative error rates).
- If error bars are reported in tables or plots, The authors should explain in the text how they were calculated and reference the corresponding figures or tables in the text.

8. **Experiments Compute Resources**

   Question: For each experiment, does the paper provide sufficient information on the computer resources (type of compute workers, memory, time of execution) needed to reproduce the experiments?

   Answer: [Yes]

   Justification: We leave these details in App. A.2.

   Guidelines:

   - The answer NA means that the paper does not include experiments.
   - The paper should indicate the type of compute workers CPU or GPU, internal cluster, or cloud provider, including relevant memory and storage.
   - The paper should provide the amount of compute required for each of the individual experimental runs as well as estimate the total compute.
   - The paper should disclose whether the full research project required more compute than the experiments reported in the paper (e.g., preliminary or failed experiments that didn't make it into the paper).

9. **Code Of Ethics**

   Question: Does the research conducted in the paper conform, in every respect, with the NeurIPS Code of Ethics `https://neurips.cc/public/EthicsGuidelines`?

   Answer: [Yes]

   Justification: We have followed all the listed NeurIPS Code of Ethics.

   Guidelines:

   - The answer NA means that the authors have not reviewed the NeurIPS Code of Ethics.
   - If the authors answer No, they should explain the special circumstances that require a deviation from the Code of Ethics.
   - The authors should make sure to preserve anonymity (e.g., if there is a special consideration due to laws or regulations in their jurisdiction).

10. **Broader Impacts**

    Question: Does the paper discuss both potential positive societal impacts and negative societal impacts of the work performed?

    Answer: [Yes]

    Justification: We discuss these in App. E.1.

    Guidelines:

    - The answer NA means that there is no societal impact of the work performed.
    - If the authors answer NA or No, they should explain why their work has no societal impact or why the paper does not address societal impact.
    - Examples of negative societal impacts include potential malicious or unintended uses (e.g., disinformation, generating fake profiles, surveillance), fairness considerations (e.g., deployment of technologies that could make decisions that unfairly impact specific groups), privacy considerations, and security considerations.

https://doi.org/10.52202/079017-4102

- The conference expects that many papers will be foundational research and not tied to particular applications, let alone deployments. However, if there is a direct path to any negative applications, the authors should point it out. For example, it is legitimate to point out that an improvement in the quality of generative models could be used to generate deepfakes for disinformation. On the other hand, it is not needed to point out that a generic algorithm for optimizing neural networks could enable people to train models that generate Deepfakes faster.
- The authors should consider possible harms that could arise when the technology is being used as intended and functioning correctly, harms that could arise when the technology is being used as intended but gives incorrect results, and harms following from (intentional or unintentional) misuse of the technology.
- If there are negative societal impacts, the authors could also discuss possible mitigation strategies (e.g., gated release of models, providing defenses in addition to attacks, mechanisms for monitoring misuse, mechanisms to monitor how a system learns from feedback over time, improving the efficiency and accessibility of ML).

11. **Safeguards**

    Question: Does the paper describe safeguards that have been put in place for responsible release of data or models that have a high risk for misuse (e.g., pretrained language models, image generators, or scraped datasets)?

    Answer: [NA]

    Justification: To the best of our knowledge, the pretrained CLIP model does not have any such associated high risk.

    Guidelines:

    - The answer NA means that the paper poses no such risks.
    - Released models that have a high risk for misuse or dual-use should be released with necessary safeguards to allow for controlled use of the model, for example by requiring that users adhere to usage guidelines or restrictions to access the model or implementing safety filters.
    - Datasets that have been scraped from the Internet could pose safety risks. The authors should describe how they avoided releasing unsafe images.
    - We recognize that providing effective safeguards is challenging, and many papers do not require this, but we encourage authors to take this into account and make a best faith effort.

12. **Licenses for existing assets**

    Question: Are the creators or original owners of assets (e.g., code, data, models), used in the paper, properly credited and are the license and terms of use explicitly mentioned and properly respected?

    Answer: [Yes]

    Justification: We have provided citations wherever necessary.

    Guidelines:

    - The answer NA means that the paper does not use existing assets.
    - The authors should cite the original paper that produced the code package or dataset.
    - The authors should state which version of the asset is used and, if possible, include a URL.
    - The name of the license (e.g., CC-BY 4.0) should be included for each asset.
    - For scraped data from a particular source (e.g., website), the copyright and terms of service of that source should be provided.
    - If assets are released, the license, copyright information, and terms of use in the package should be provided. For popular datasets, `paperswithcode.com/datasets` has curated licenses for some datasets. Their licensing guide can help determine the license of a dataset.
    - For existing datasets that are re-packaged, both the original license and the license of the derived asset (if it has changed) should be provided.

- If this information is not available online, the authors are encouraged to reach out to the asset's creators.

13. **New Assets**

    Question: Are new assets introduced in the paper well documented and is the documentation provided alongside the assets?

    Answer: [NA]

    Justification: We do not release any new assets.

    Guidelines:

    - The answer NA means that the paper does not release new assets.
    - Researchers should communicate the details of the dataset/code/model as part of their submissions via structured templates. This includes details about training, license, limitations, etc.
    - The paper should discuss whether and how consent was obtained from people whose asset is used.
    - At submission time, remember to anonymize your assets (if applicable). You can either create an anonymized URL or include an anonymized zip file.

14. **Crowdsourcing and Research with Human Subjects**

    Question: For crowdsourcing experiments and research with human subjects, does the paper include the full text of instructions given to participants and screenshots, if applicable, as well as details about compensation (if any)?

    Answer: [NA]

    Justification: We do not rely on crowdsourcing experiments.

    Guidelines:

    - The answer NA means that the paper does not involve crowdsourcing nor research with human subjects.
    - Including this information in the supplemental material is fine, but if the main contribution of the paper involves human subjects, then as much detail as possible should be included in the main paper.
    - According to the NeurIPS Code of Ethics, workers involved in data collection, curation, or other labor should be paid at least the minimum wage in the country of the data collector.

15. **Institutional Review Board (IRB) Approvals or Equivalent for Research with Human Subjects**

    Question: Does the paper describe potential risks incurred by study participants, whether such risks were disclosed to the subjects, and whether Institutional Review Board (IRB) approvals (or an equivalent approval/review based on the requirements of your country or institution) were obtained?

    Answer: [NA]

    Justification: We do not use human subjects for research in this work.

    Guidelines:

    - The answer NA means that the paper does not involve crowdsourcing nor research with human subjects.
    - Depending on the country in which research is conducted, IRB approval (or equivalent) may be required for any human subjects research. If you obtained IRB approval, you should clearly state this in the paper.
    - We recognize that the procedures for this may vary significantly between institutions and locations, and we expect authors to adhere to the NeurIPS Code of Ethics and the guidelines for their institution.
    - For initial submissions, do not include any information that would break anonymity (if applicable), such as the institution conducting the review.

 https://doi.org/10.52202/079017-4102